Miocene detachment faulting predating EPR propagation: Southern Baja California

Anna Bot, Laurent Geoffroy, Christine Authemayou, Hervé Bellon, David Graindorge, Raphaël Pik

AGU PUBLICATIONS

Tectonics

RESEARCH ARTICLE
10.1002/2015TC004030

Key Points:
- An unrecognized detachment fault allowed the opening of the San Jose del Cabo Basin
- The detachment fault accommodated the crustal necking with a N118E trending sigma3
- The detachment fault activity occurred from approximately 13 to 5 Ma, predating the EPR propagation

Supporting Information:
- Supporting Information S1
- Table S1
- Table S2

Correspondence to:
A. Bot,
anna.bot@univ-brest.fr

Citation:
Bot, A., L. Geoffroy, C. Authemayou, H. Bellon, D. Graindorge, and R. Pik (2016), Miocene detachment faulting predating EPR propagation: Southern Baja California, *Tectonics*, *35*, 1153–1176, doi:10.1002/2015TC004030.

Received 14 SEP 2015
Accepted 22 APR 2016
Accepted article online 27 APR 2016
Published online 20 MAY 2016

Miocene detachment faulting predating EPR propagation: Southern Baja California

Anna Bot[1], Laurent Geoffroy[1], Christine Authemayou[1], Hervé Bellon[1], David Graindorge[1], and Raphaël Pik[2]

[1]LDO, UMR 6538, Université de Bretagne Occidentale, IUEM, Plouzané, France, [2]CRPG, UMR 7358, Université de Lorraine-CNRS, Nancy, France

Abstract At the southern tip of the Baja California peninsula, we characterize the onshore structures and kinematics associated with crustal necking leading up to the Pliocene breakup and early East Pacific Rise seafloor spreading. From a combination of tectonic field investigations, K-Ar and cosmogenic isotope dating and geomorphology, we propose that the Los Cabos block represents the exhumed footwall of a major detachment fault. This north trending detachment fault is marked by a conspicuous low-dipping brittle-ductile shear zone showing a finite displacement with top to the SE ending to the ESE. This major feature is associated with fluid circulations which led to rejuvenation of the deformed Cretaceous magmatic rocks at a maximum of 17.5 Ma. The detachment footwall displays kilometer-scale corrugations controlling the present-day drainage pattern. This major detachment is synchronous with the development of the San José del Cabo Basin where syntectonic sedimentation took place from the middle Miocene to probably the early Pliocene. We propose that this seaward dipping detachment fault accommodates the proximal crustal necking of the Baja California passive margin, which predates the onset of formation of the East Pacific Rise spreading axis in the Cabo-Puerto Vallarta segment. Our data illustrate an apparent anticlockwise rotation of the stretching direction in Baja California Sur from ~17 Ma to the Pliocene.

1. Introduction

The stress and strain fields prevailing during oblique rifting and consecutive breakup are poorly constrained. Most studies focus on experimental modeling. A number of these experiments reproduce the patterns of faulting developed at upper crustal, bulk crustal, or lithospheric scales when divergence occurs at $<90°$ relative to an (inherited) mechanical discontinuity [e.g., *Autin et al.*, 2010a; *Brune*, 2014]. Concerning the specific topic of oblique rifting, the modeling clearly needs to be better constrained by further observational data describing the evolution in space and time of strain in developing oblique extensional systems. There are indeed few passive margins where it is possible to describe in detail the finite geometry of oblique rifting and the evolution of deformation with time [e.g., *Fournier et al.*, 2004; *Leroy et al.*, 2012; *Autin et al.*, 2013; *Bellahsen et al.*, 2013a; *Pik et al.*, 2013]. In particular, there is little understanding of the 3-D finite architecture of successive sedimentary basins developing over major normal faults with different orientations. This aspect appears to be a key to understanding the complexity of nested basins formed in oblique to transform-like settings. Here we present new data from Baja California which improve our knowledge about the geometry of basins developing in the framework of a highly oblique extensional system.

The NNW trending Gulf of California (GOC) forms an oblique boundary between the Pacific and the North America plates, connecting the San Andreas fault in the north to the East Pacific Rise (EPR) farther south (Figure 1). It consists of a pull-apart system of short en echelon NE trending spreading segments which are subordinate to long NW trending dextral transform faults [*Lonsdale*, 1989] trending parallel to the present-day plate motion vector [e.g., *Plattner et al.*, 2009]. The relative divergent motion between the Pacific and North America plates was relatively constant from 30 to 8 Ma according to a N120°E trend. From 8 Ma, the motion vector became reoriented along a N143°E direction [*Atwater and Stocks*, 1998].

The continental breakup and incipient oceanization occurred between 3 and 3.5 Ma along the Alarcon Rise (Figure 1b) [*Demets*, 1995]. According to *Lonsdale* [1989], an aborted phase of early oceanic spreading started in the southernmost Cabo/Puerto-Vallarta segment (Maria Magdalena Rise, Figure 1a) at 4.5 Myr, i.e., ~1 Ma before the main northeastward propagation of the East Pacific Rise [*DeMets*, 1995] (Figure 1). The age of true oceanic crust (if any) and, thus, the age of breakup, is unknown for the short divergent segments located farther north within the GOC itself.

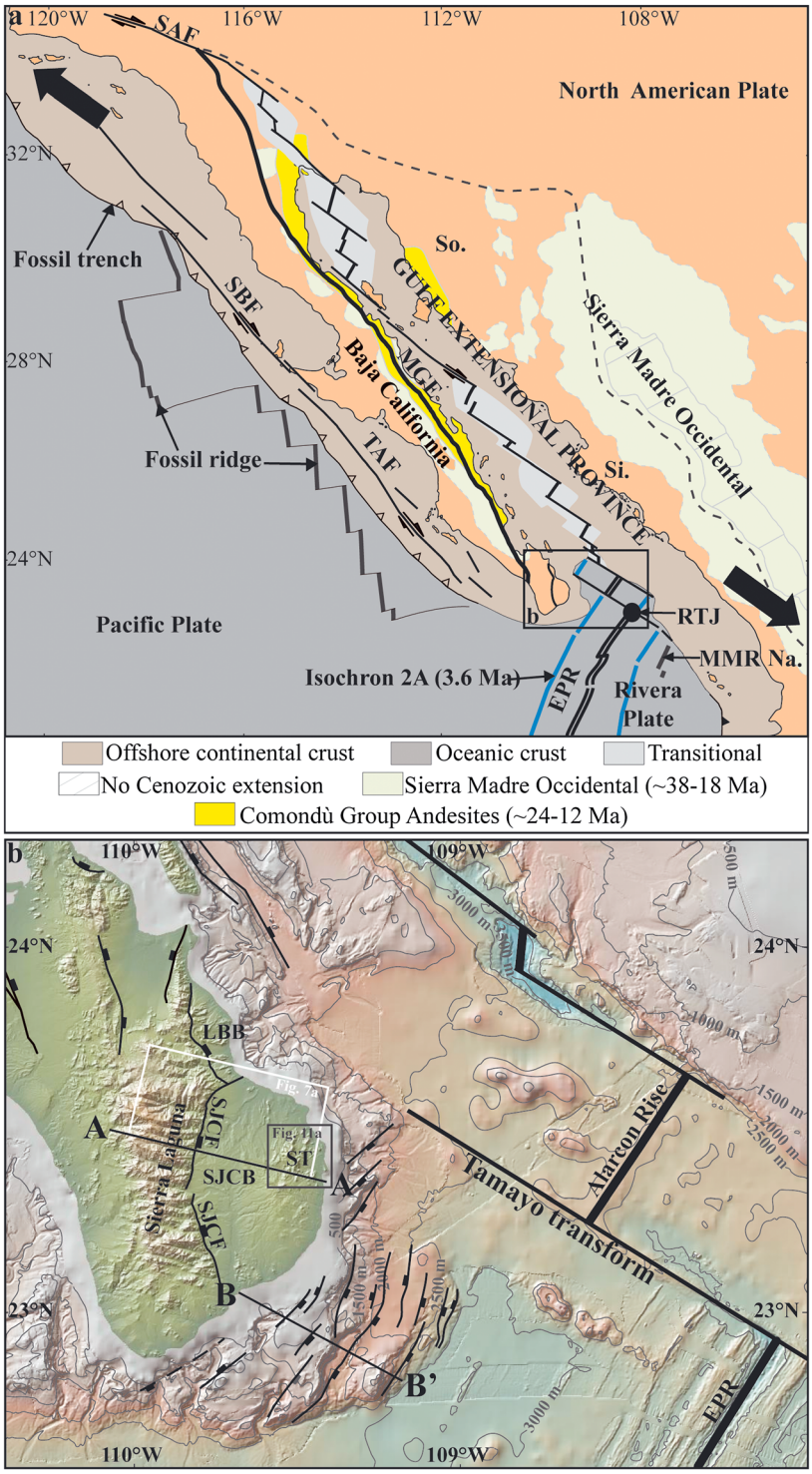

Figure 1. (a) Tectonic map of the Gulf of California region. Volcanic formations contours are from *Bryan et al.* [2014], GEP contour are from *Axen* [1995], and offshore structures are from *Lonsdale* [1991]. TAF: Tosco-Abreojos fault, SBF: San Benito fault, EPR: East Pacific Rise, MGE: Main Gulf Escarpment, MMR: Maria Magdalena Rise, RTJ: Riviera Triple Junction, Na.: Nayarit, Si.: Sinaloa, and So.: Sonora. Black arrows indicate the current relative plate motion [*Plattner et al.*, 2009]. (b) Shaded relief map of Los Cabos area. The offshore faults are located after *Curray et al.* [1982]. AA' and BB' lines show locations of cross sections on Figure 11, the white box indicates the area of the geological map on Figure 10a, and the grey box indicates area of map on Figure 12a. Digital elevation model was created using *GeoMapApp* (http://www.GeoMapApp.org). ST: Sierra La Trinidad, SJCB: San José del Cabo Basin, LBB: Los Barriles Basin, SJCF: San José del Cabo fault, and SJPF: San Juan de Los Planes fault.

From the Late Cretaceous to the Miocene, the Baja California/Sierra Madre Occidental area consisted of a magmatic arc developed above the Farallon Plate subduction zone [e.g., *Karig and Jensky*, 1972; *Hausback*, 1984; *Ferrari et al*., 2007]. From the end of the subduction process (at ~12.5 Ma) [*Lonsdale*, 1989], it is generally proposed that the oblique divergence during continental stretching and thinning was partitioned. From 12 to 6 Ma, dextral shearing occurred on the western edge of the Peninsula along the WNW trending San Benito and Tosco-Abreojos strike-slip faults [*Spencer and Normark*, 1979; *Lonsdale*, 1991] (Figure 1a), while NE to ENE trending pure extension took place along NW-SE trending faults bounding the GOC. The related extensional zone, called the Gulf Extensional Province or GEP [*Gastil et al*., 1975; *Stock and Hodges*, 1989] (Figure 1a), is focused on the Gulf of California area: it is bounded to the west by the Main Gulf Escarpment (MGE) in Baja California and extends eastward to the Sierra Madre Occidental (Figure 1a). As described further below, these NW trending extensional structures are suborthogonal to the regional minimum stress vector computed from the inversion of fault slip data set [*Angelier et al*., 1981; *Colletta and Angelier*, 1983] and are subparallel to and superimposed onto the Paleogene to Miocene volcanic arc. This configuration suggests a causal relationship between the overthickened arc-related crust and a possible gravity-driven extensional collapse [e.g., *Liu*, 2001; *Lewis et al*., 2001]. In the eastern part of the GEP, this pure NE to ENE trending extension is well documented from 25 Ma onward in the Sonora area (Figure 1a), producing low-dipping detachment faults associated with core complexes. This activity continued until 15 Ma [*Nourse et al*., 1994; *Wong and Gans*, 2003, 2008; *Wong et al*., 2010], followed by high-angle faulting until 10 Ma [*Gans*, 1997]. According to different authors, extension began farther south in the Sinaloa and Nayarit areas (Figure 1a) between 17 and 11 Ma [*Henry and Aranda-Gomez*, 2000] or between 12 and 9 Ma [e.g., *Henry and Aranda-Gomez*, 2000]. To the west, along the Baja California peninsula, the NW trending Main Gulf Escarpment (Figure 1a) represents the breakaway zone of a major detachment fault system segmented by transfer faults [*Axen*, 1995; *Drake*, 2005]. Fault slip data recorded throughout central and southern Baja California indicate that the minimum stress σ_3 trended N060°E to N080°E and was suborthogonal to the Main Gulf Escarpment [*Angelier et al*., 1981; *Colletta and Angelier*, 1983]. Tectonic activity in the northern part of the Main Gulf Escarpment [*Seiler et al*., 2011] began at 9–7 Ma, but earlier extensional deformation, at 16–10 Ma [*Lee et al*., 1996] or 12.5–6 Ma [*Lewis and Stocks*, 1998], is also documented in the same area. In the central part of the peninsula, this major suborthogonal extensional deformation is bracketed between 11 and 5 Ma [*Angelier et al*., 1981; *Colletta and Angelier*, 1983; *Zanchi*, 1994]. This is consistent with the age of the Los Barriles detachment fault [*Geoffroy et al*., 2009; *Geoffroy and Pronost,* 2010; *Masini et al*., 2010], which is now dated as older than 5 Ma (this study).

Since ~6 Ma, the main deformation appears to have become localized in the present-day oceanic GOC [*Oskin et al*., 2001; *Oskin and Stock*, 2003a, 2003b]. However, part of this deformation is still active and would be accommodated along the Tosco-Abreojos fault (Figure 1a) [*Michaud et al*., 2004] and across the Baja California continental margin [*Munguía et al*., 2006].

Some authors [*Gans*, 1997; *Fletcher et al*., 2007; *Seiler et al*., 2010] question the amount of finite dextral displacement along the western edge of Baja California and hence the amount of strain partitioning during continental extension, proposing that deformation in the GEP has been accommodated by dextral transtensive shearing since 12.5 Ma ago.

To elucidate the origin and tectonic evolution of the GOC, a major issue to be addressed is related to the strain field associated with the northeastward reorientation and propagation of the EPR across the present-day Baja California Peninsula following the extinction of the NNE-SSW trending Maria Magdalena Rise at ~4.5 Ma [see *Lonsdale*, 1989, Figures 8 and 10] (Figure 1a). The specific continental extensional strain field predating the propagation of the northeastward EPR ridge has never been clearly described, and no explanation has so far been proposed for its timing and relation with the pure extensional strain field affecting the GEP since the Miocene. The formation of a continental passive margin predating the EPR propagation has been revealed by a combination of seismic and gravity data along the "Cabo-PV" profile acquired during the Pescador experiment [*Lizarralde et al*., 2007; *Páramo et al*., 2008]. These authors [*Lizarralde et al*., 2007; *Páramo et al*., 2008] proposed that the ~75 km width passive margin is nonmagmatic, being associated with a significant crustal necking from the approximate location of the San José del Cabo fault at the southern tip of the Baja California peninsula (Figure 1b). The minimum age for this tectonic thinning is indirectly constrained from the first (postdating) seafloor magnetic anomalies of the EPR, i.e., 2A (i.e., ~3.6 Ma) [*DeMets*, 1995] offshore SE Baja California (Figure 1). In the Alarcon segment, north of the Tamayo transform (Figure 1b), *Sutherland et al*. [2012] infer

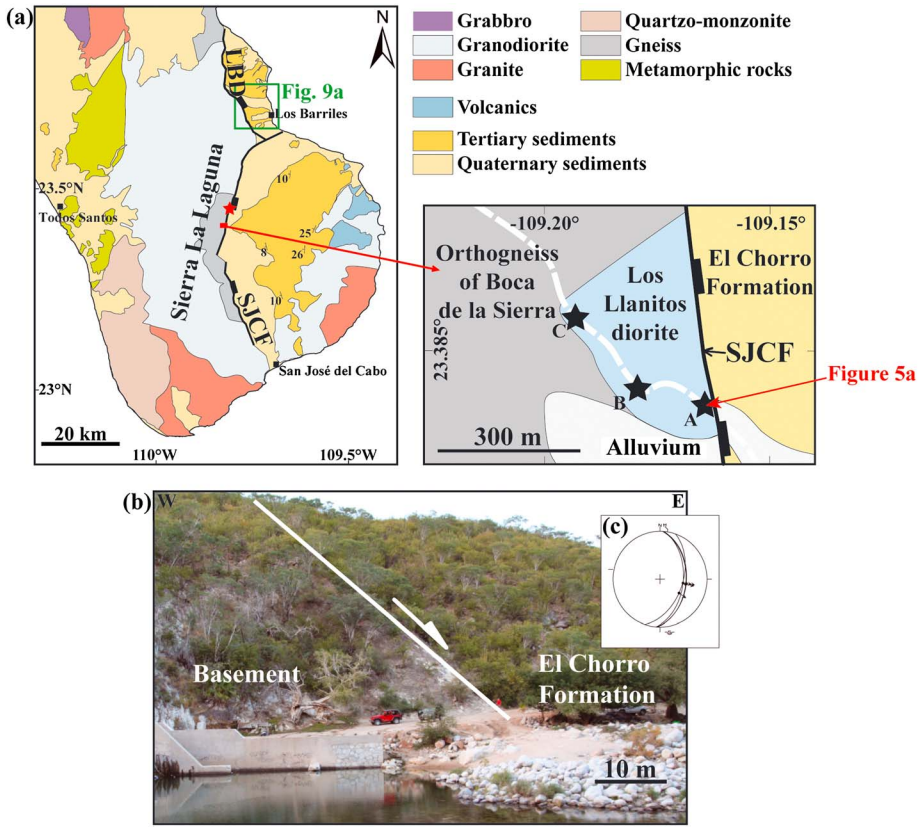

Figure 2. (a) Simplified geological map of the Los Cabos area modified from *Pérez-Venzor* [2013] and *Romero et al*. [2002] with a zoom view on the site of the Los Cabos detachment outcrop showing sample locations for K-Ar dating (Stars = A: GOC04 and GOC05; B: GOC06 and GOC07; C: GOC08 and GOC09). LBD: Los Barriles detachment and SJCF: San José del Cabo fault. (b) View of the San José del Cabo fault (23°26.4′N; 109°48.47′W). (c) Stereogram (lower hemisphere projection) of the San José del Cabo fault-related fault plane with striae (same location as Figure 2b).

an early continental NW trending extension episode beginning around ~14–11 Ma based on sedimentation rates in syntectonic basins formed in connection with offshore faults trending NE-SW [*Sutherland*, 2006].

Although a substantial part of the crustal thinning probably occurred onshore at the southern extremity of the Baja California Peninsula, the geometry and fault pattern of this deformation is poorly described in the upper crust (see next section). Offshore, *Curray et al*. [1982] and *Páramo et al*. [2008] identified an array of predominantly southeast dipping normal faults bounding small-scale undated syntectonic basins.

In the present study, using a combination of tectonic, geomorphic, and radiometric age data, we characterize the onshore expression of the margin crustal necking, as illustrated by *Páramo et al*. [2008], which ended with Pliocene breakup and early EPR seafloor spreading at the southernmost extremity of the Baja California peninsula. We discuss the significance of the related strain and stress field in the general framework of the opening of the GOC.

2. Geological Setting

A range and basin topography with ~N-S trending structures characterizes the southern tip of the Baja California Peninsula (Figures 1b and 2a). The Miocene to Quaternary San José del Cabo Basin (SJCB) is bounded to the east by the Sierra La Trinidad (ST), mainly composed of Cretaceous intrusive rocks locally covered by Miocene acidic volcanics [*Lyle and Ness*, 1991; *Martínez-Gutiérrez and Sethi*, 1997]. To the west, the San José del Cabo Basin is bounded by the Sierra La Laguna (SL) or Los Cabos Block (Figures 1b and 2a) [*Schaaf et al*., 2000], where a major intrusive suite of tonalitic-quartz-dioritic granitoids yields Rb-Sr ages of 115 ± 4 Ma and a biotite cooling age of 90 ± 2 Ma (Figure 2a) [*Schaaf et al*., 2000]. These granitoids are intruded into older metasedimentary and metaigneous rocks of Mesozoic age. More recent intrusive bodies

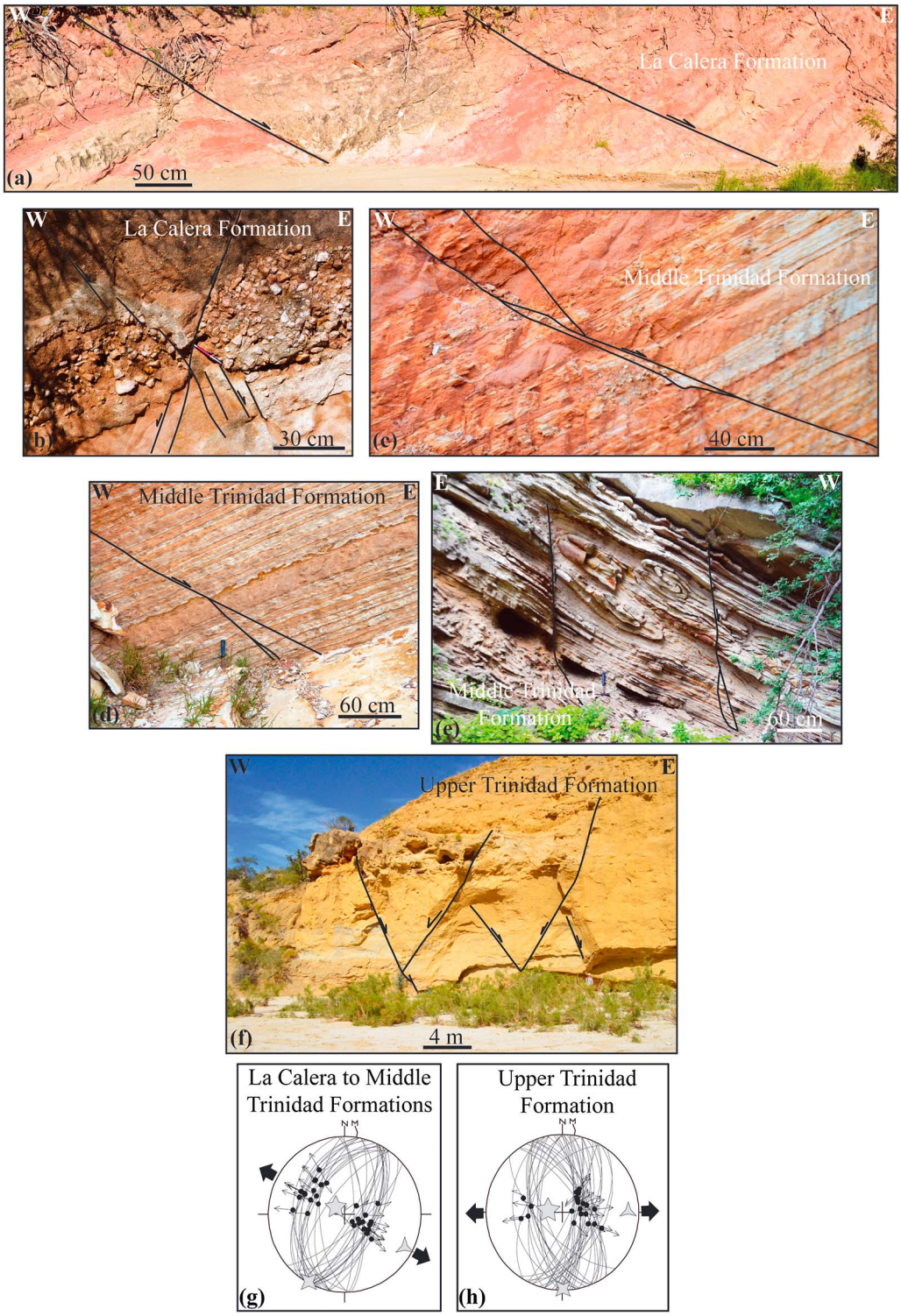

Figure 3. (a–e) Examples of synsedimentary tilted faults in the La Calera formation (23°24.26′N; 109°35.51′W, Figures 3a and 3b) and in diatomite beds belonging to the Middle Trinidad formation ([23°21.76′N; 109°36.65′W] Figures 3c and 3d and [23°21.72′N; 109°36.68′W] Figure 3e) with probable paleosismite (Figure 3d) and tilted syndeposition normal faults sealed by sediments and syntectonic sediment deformation slump features (Figure 3e). (f) Conjugate faults affecting the Upper Trinidad formation (23°25.15′N; 109°38.85′W). (g) Untilted fault slip data and associated stress tensors recorded in the La Calera to Middle Trinidad formations with a minimum stress σ_3 trending N118°E (lower hemisphere projection). (h) Fault slip data and associated stress tensors recorded in the Upper Trinidad formation with σ_3 trending N088°E (lower hemisphere projection).

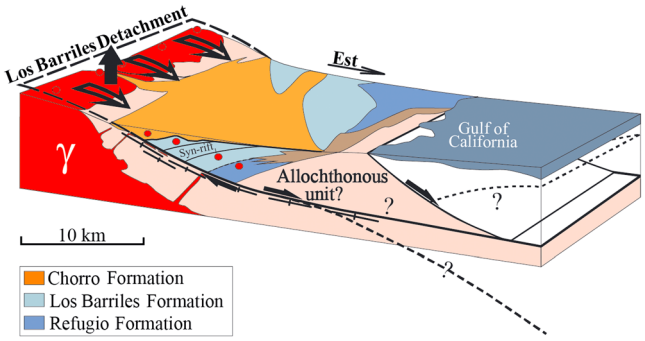

Figure 4. The Los Barriles detachment fault, according to *Geoffroy and Pronost* [2010] modified by *Geoffroy et al.* [2009].

such as diorites (78 to 58 Ma) have been detected to the east of the Sierra La Laguna [*Pérez-Venzor*, 2013]. The Los Cabos Block is bounded to the east by the east dipping San José Del Cabo normal fault (SJCF; Figures 2a and 2b). This fault is described as high angle [*Fletcher et al.*, 2000]. The San José del Cabo fault locally cuts Quaternary alluvial deposits ("El Chorro formation") [see *Martínez-Gutiérrez and Sethi*, 1997] and was recently reactivated in its southern part [*Fletcher and Munguia*, 2000].

The San José del Cabo Basin (Figures 1b and 2a) was considered as an asymmetric graben basin controlled to the west by the San José del Cabo fault [*Martínez-Gutiérrez and Sethi*, 1997; *Fletcher et al.*, 2000; *Busch et al.*, 2011]. Its infilling consists in middle Miocene to Pleistocene continental and marine sediments [*Martínez-Gutiérrez and Sethi*, 1997] deposited on crystalline bedrock down to 2.7 km depth [*Busch et al.*, 2011]. Its origin is associated with the opening of the GOC [*McCloy*, 1984; *Martínez-Gutiérrez and Sethi*, 1997; *McTeague et al.*, 2005]. *Martínez-Gutiérrez and Sethi* [1997] have established and formally defined the stratigraphy of the San José del Cabo Basin and have tentatively proposed some ages. The lowermost sedimentary unit, the La Calera formation, corresponds to conglomerates and sandstones (Figures 3a and 3b) of presumed middle Miocene to upper Miocene age. It is overlain by the Trinidad formation, a conformable transgressive unit characterized by lateral changes of lithology from the south to north across the basin. *Martínez-Gutiérrez and Sethi* [1997] suggest late Miocene to Early Pliocene age, and *McTeague et al.* [2006] estimate that the lower member of the Trinidad formation was deposited beginning from 9 to 13 Ma ago based on sedimentation rates and foraminifera and coccoliths. The fauna-rich lowermost facies is composed of shales, siltstones, and sandstones. The middle facies represents a deeper depositional environment with siltstones and muddy sandstones containing diatomite beds (Figures 3c–3e). It is also characterized by slumps often faulted controlled mainly observed in the muddy sandstones (Figure 3e). The upper facies reflects shallow marine conditions with deposition of cross-bedded sandstones and siltstones containing shell fragments (Figure 3f). The regressive deposits of the overlying Refugio formation (considered as early Pliocene to late Pliocene) are composed of sandstones interbedded with fossiliferous limestones and shales, passing progressively upward (and also laterally) into the continental Los Barriles formation at the top which consists of sandstones and conglomerates containing submetric to metric boulders. In the northern part of the basin, and near the San José del Cabo fault, *Arreguín-Rodríguez and Schwennicke* [2013] describe some evidence of interfingering between the Los Barriles and Trinidad formations that implies their coeval deposition, probably during the Pliocene, which would modify the chronology established by *Martínez-Gutiérrez and Sethi* [1997].

Finally, the widespread upper Pleistocene to Holocene continental El Chorro formation is a classical fan deposit which unconformably overlies the older strata [*Martínez-Gutiérrez and Sethi*, 1997], representing everywhere a postrift deposit.

Toward the north, the Los Barriles Basin (Figure 1b), distinct from the San José del Cabo Basin, developed subsequent to tectonic collapse of the Los Cabos Block following a NE trend along the Los Barriles detachment fault (Figure 4). *Geoffroy et al.* [2009] and *Geoffroy and Pronost* [2010] and *Masini et al.* [2010] clearly show that the Los Barriles and Refugio formations were syntectonic with respect to the Los Barriles detachment fault (Figure 3).

3. Tectonics, Uplift, and Sedimentation in Southern Baja California Sur

3.1. The Boca de la Sierra Shear Zone

According to previous studies, the San José del Cabo fault appears to represent the dominant fault of the region since the middle to late Miocene, being the major structure controlling the development of the San José del Cabo Basin [e.g., *Fletcher and Munguia*, 2000].

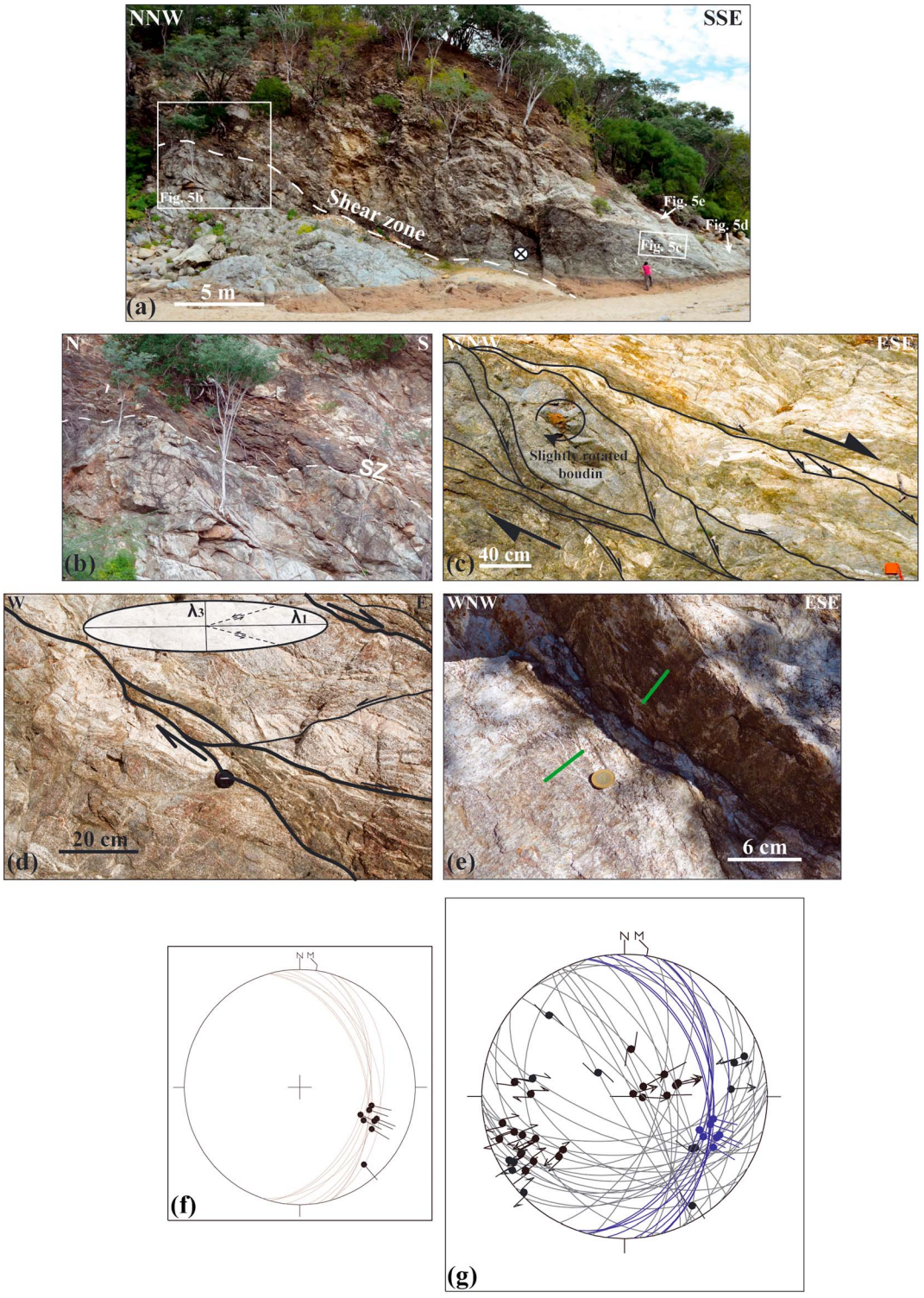

Figure 5. The Boca de la Sierra site. (a) View of the Los Cabos detachment and the associated brittle-ductile shear zone (location on Figure 2a). (b) Zoom views on the shear zone (location on Figure 5a). (c) Zoom views of shear zone structures with boudinaged structures (location in Figure 5a). (d) Zoom views of shear zone structures with transposed intrusions (location in Figure 5a) and interpreted deformation ellipsoid. (e) Zoom views of brittle structures in the shear zone with ubiquitous syntectonic chlorite (location in Figure 3a); the green features represent the slips on the faults planes. (f) The foliation and the mineral lineation associated on shear planes. The mean value corresponding to the N115°E ± 5° extension compatible with the semiductile stretching direction inferred from the boudinage structures (lower hemisphere projection). (g) Relation between lineation of ductile structures and fault slips of late shear planes and minor brittle faults with ubiquitous syntectonic chlorite.

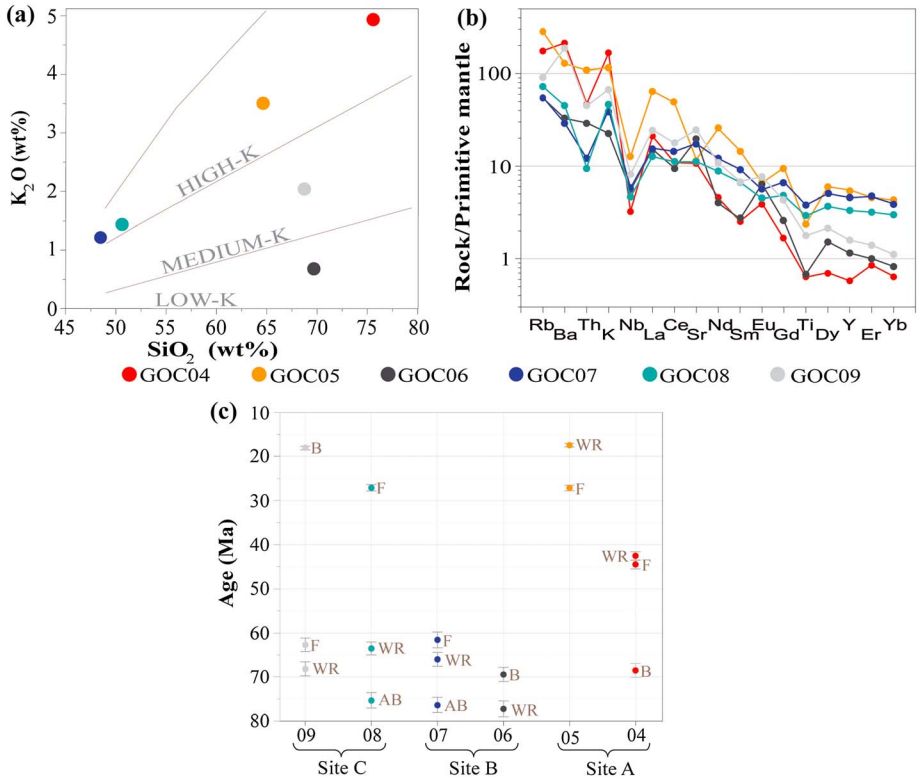

Figure 6. (a) K_2O-SiO_2 plot for GOC04 to GOC09 samples according to *Peccerillo and Taylor* [1976] (locations on Figure 2a). (b) Incompatible multielement pattern of same samples normalized to Primitive Mantle [*Sun and McDonough*, 1989]. (c) K-Ar dating on whole rocks (WR) and separated minerals (AB: Amphibole and Biotite and F: Feldspar (plagioclase)) of samples 04 to 09 (corresponding to GOC04 to GOC09 on Figure 2a).

It is important to note that in contradistinction to *Fletcher and Munguia* [2000], we consider that the low-dipping Los Barriles detachment fault (Figures 1b and 4) [*Geoffroy et al.*, 2009; *Geoffroy and Pronost*, 2010; *Masini et al.*, 2010] is not the northwestward continuation of the San José del Cabo fault (see section 4). However, our observations on the San José del Cabo fault, as illustrated on Figure 2b, suggest that the dip angle of this fault could be as low as 45°, at least locally (Figure 2c). This fault shows no significant cataclastic deformation at its footwall and locally displays tectonic slickensides striking N090°E to N120°E (Figure 2c). It is noteworthy that while these observations are quite clear, they are insufficiently numerous to characterize the entire tectonic history of this fault. We propose hereafter that this fault crosscut a major ductile to cataclastic low-dipping shear zone.

Here we especially study the contact between the basin sediments and the basement at the Boca de la Sierra site (Figures 2a and 5). This site locally exposes the Los Llanitos diorite, of ~90 to 78 Ma (Figure 2a) [*Pérez-Venzor*, 2013], which is intruded by a number of nondated acid planar intrusions, predominantly dikes. The Los Llanitos diorite displays a clear magmatic fabric without any superposed significant solid-state (plastic) deformation. However, at the footwall of the San José del Cabo fault, there is a >10 m wide ductile to cataclastic extensional shear zone dipping ~20° to the SE which reworks and transposes the initial magmatic fabric (Figures 5a and 5b). All previous dikes are transposed and intensely stretched, showing boudinage structures within the shear zone (Figures 5c and 5d) which is otherwise characterized by a penetrative ductile-to-brittle planar fabric (Figure 5d). The associated kinematic direction is dominantly ~ N115°E ± 5° (Figure 5f) top to the east. The shear zone itself appears to be slightly corrugated along strike. Late shear planes and minor brittle faults with ubiquitous syntectonic chlorite (Figure 5e) crosscut the main shear zone with apparent extension direction parallel to the E-W to NE-SW trend (before any untilting of those faults; Figure 5g).

Six samples (GOC04 to GOC09) were analyzed for major and trace element geochemistry as well as K-Ar dating on whole rocks and separated minerals (Figures 2a and 6 and Tables 1 and 2; K-Ar method is explained

Table 1. Geochemical Analyses of Samples GOC04 to 09 (for Location: See Figure 2a)

Sample	GOC07	GOC08	GOC05	GOC09	GOC06	GOC04
Rock type	Diorite	Diorite	Granodiorite	Granitic Dike	Granitic Dike	Granite
			Major Elements (wt %)			
SiO_2	48.48	50.61	64.63	68.72	69.68	75.55
TiO_2	0.83	0.63	0.52	0.39	0.15	0.14
Al_2O_3	16.88	11.54	15.40	16.32	17.42	12.86
Fe_2O_3	9.22	9.74	4.64	2.60	1.35	0.89
MnO	0.17	0.14	0.08	0.03	0.03	0.02
MgO	8.26	13.21	1.02	1.00	0.66	0.30
CaO	10.73	8.21	3.05	3.86	4.90	1.34
Na_2O	1.48	1.22	4.49	3.84	4.48	2.98
K_2O	1.22	1.44	3.51	2.04	0.68	4.94
P_2O_5	0.15	0.10	0.17	0.13	0.06	0.04
LOI	1.33	1.76	1.96	0.65	0.40	1.00
Total	98.74	98.64	99.47	99.57	99.80	100.05
			Trace Elements (ppm)			
Rb	34.51	46.17	178.07	57.22	34.72	111.16
Ba	203.60	313.42	881.48	1329.25	229.30	1513.04
Th	1.03	0.82	9.24	3.80	2.49	4.02
Nb	4.13	3.25	8.95	5.82	3.90	2.36
La	10.76	8.71	44.58	17.21	10.46	13.98
Ce	26.21	20.48	82.09	31.91	17.73	20.19
Sr	370.07	235.22	248.50	529.36	410.92	225.72
Nd	16.42	11.85	34.57	14.60	5.42	6.03
Sm	3.99	2.97	6.51	3.02	1.20	1.13
Zr	26.58	22.84	26.83	16.85	9.11	29.11
Eu	0.94	0.75	1.11	1.27	1.07	0.67
Gd	4.00	2.87	5.70	2.51	1.54	0.98
Dy	3.72	2.72	4.40	1.58	1.13	0.52
Y	20.76	15.18	25.19	7.24	5.23	2.63
Er	2.24	1.54	2.20	0.68	0.48	0.41
Yb	1.94	1.47	2.12	0.55	0.41	0.32
Sc	37.39	31.53	14.74	5.51	3.83	2.53
V	262.34	203.06	53.81	34.19	21.66	13.66
Cr	306.12	334.13	9.14	14.75	7.82	7.39
Co	30.36	49.53	6.69	5.19	2.97	1.10
Ni	20.11	35.04	2.58	2.21	1.79	0.93

in the footnote of Table 2). Four samples were collected in the Los Llanitos diorite away from the shear zone (sites B and C on Figure 2a) comprising two high K basic diorites (GOC07 and 08) and two crosscutting granitic dikes with low K (GOC06) and medium K (GOC09) (Figure 6a and Table 1). Finally, two samples (a granite, GOC04, and a granodiorite, GOC05) were collected within the shear zone itself (site A on Figure 2a). All samples are relatively fresh, with Loss On Ignition values lower than 2 wt % (Table 1), even if intense fluid circulation is suspected, as discussed further below. All samples display extended trace element patterns with similar shapes and the presence of a negative Nb anomaly typical of arc-related rocks (Figure 6b). The shear zone is associated with a clear enrichment in potassium (Figure 6a).

The dating results show a wide spread of K-Ar ages, which more or less reflects disturbances of the whole rock systems. Two main groups of ages can be distinguished as well as a third intermediate group (Figure 6c and Table 2):

1. The ages of the first group are 77 to 75 ± 2 Ma for samples from the footwall (whole rock of granitic dike (GOC06) and amphiboles and biotites separated from the Los Llanitos diorite (GOC07 and 08)). Some younger ages (66 to 61 Ma) are determined from whole rocks and separated feldspars (plagioclases) in granitic dike (GOC09) or solely from biotites in ganite (GOC04).
2. The second group of ages younger is than 30 Ma, between 27 and 17.5 Ma, for newly crystallized biotites in granitic dike (GOC09), plagioclases in diorite (GOC08), as well as whole rock and plagioclases in granodiorite (GOC05; within the shear zone).

Table 2. ^{40}K-^{40}Ar Ages of Whole Rocks and Separated Minerals (WR: Whole Rock, AB: Amphibole and Biotite, and F: Feldspar (Plagioclases) From Samples GOC04 to 09 (for Location: See Figure 2a)[a]

	Coordinates				Age (Ma)	$^{40}Ar_R$	$^{40}Ar_R/40Ar_T$	$^{36}Ar_{exp}$	K_2O	
Sample	Latitude North	Longitude West	Rock Type	Fraction	±1σ	(10^{-7} cm^3/g)	(%)	(10^{-10} cm^3)	(wt %)	Ref. Analysis
GOC04	23°23.078′	109°49.047′	Granite	WR	42.6 ± 1.0	71.7	90.2	9.0	5.16	B7513-6
				F	44.5 ± 1.0	71.9	90.5	14.0	4.95	B7522-3
				B	68.5 ± 1.6	141.2	85.0	8.0	6.27	B7534-7
GOC05	23°23.078′	109°49.047′	Granodio-rite	WR	17.5 ± 0.4	20.3	93.2	1.3	3.59	B7511-4
				F	27.1 ± 0.6	26.3	80.2	9.9	2.99	B7543-4
GOC06	23°23.106′	109°49.149′	Granitic Dike	WR	77.2 ± 1.78	18.6	89.3	2.6	0.73	B7514-7
				B	69.4 ± 1.6	197.9	90.9	6.1	8.67	B7549-10
GOC07	23°23.106′	109°49.149′	Los Llanitosdiorite	WR	66.0 ± 1.6	23.9	65.8	14.7	1.52	B7520-1
				F	61.6 ± 1.8	4.6	39.5	13.4	0.23	B7533-6
				AB	76.4 ± 1.8	130.5	87.8	9.4	5.19	B7521-2
GOC08	23°23.205′	109°49.240′	Los Llanitosdiorite	WR	63.5 ± 1.5	32.3	85.7	6.3	1.55	B7512-5
				F	27.1 ± 0.7	8.4	49.1	7.3	0.95	B7544-5
				AB	75.3 ± 1.7	171.6	90.2	6.2	6.92	B7550-11
GOC09	23°23.205′	109°49.240′	Granitic Dike	WR	68.2 ± 1.6	38.1	81.7	9.6	1.70	B7510-3
				F	62.7 ± 1.5	24.9	63.4	27.7	1.20	B7527-8
				B	18.2 ± 0.4	51.1	72.5	6.1	8.70	B7536-9

[a] $^{40}Ar_R$: radiogenic ^{40}Ar; $^{40}Ar_T$: total ^{40}Ar; $^{36}Ar_{exp}$: ^{36}Ar of the sample. Potassium-argon ages were determined at the K-Ar dating platform of CNRS-Université de Bretagne Occidentale in Brest (France), after crushing and subsequent sieving of the solid samples to prepare grains 0.3 to 0.15 mm in size of whole rock and separated minerals (amphibole, biotite, and feldspar with quartz in the more acid rocks). One aliquot of grains was powdered in an agate grinder, providing around 0.1 g of powder subjected to chemical attack with 4 cm^3 of hydrofluoric acid, before analysis of K content by atomic absorption spectrometry. A second aliquot of grains was reserved for argon analysis. About 0.3 g to 0.8 g of grains were heated and fused under vacuum in a molybdenum crucible, using a high-frequency generator. The gases released during this step were cleaned successively on three quartz traps containing a titanium sponge, with temperature decreasing from 800°C to ambient during 10 min; at the final step, the remaining gas fraction was ultrapurified with an Al-Zr SAES getter. Isotopic composition of argon and concentration of $^{40}Ar_R$ were measured in a stainless steel mass spectrometer with a 180° geometry. Isotopic dilution was performed along with the fusion step, using precise concentrations of ^{38}Ar buried as ions in aluminum targets [*Bellon et al.*, 1981]. The resulting ages listed in Table 2 are calculated using the decay constants and errors recommended by *Steiger and Jäger* [1977], following the equation of *Cox and Dalrymple* [1967].

3. The third group concerns a cluster of results with intermediate ages around 42–44 Ma for whole rock and plagioclases in granite (GOC04; within the shear zone).
4. We assume that the oldest ages of ~77 Ma represent the age of cooling of the igneous rocks following the crystallization in-so-far as the ages are concordant with Rb-Sr dating results obtained from other diorites in the same area [*Pérez-Venzor*, 2013]. Together with the other diorite outcrops in the eastern part of the Los Cabos Block, the Los Llanitos diorite appears to represent an arc-related Late Cretaceous/Paleocene intrusion emplaced within the main Cretaceous batholith [*Pérez-Venzor*, 2013].

We observe an apparent whole rock "rejuvenation" (nonweathering alteration) for both samples collected from the shear zone which is also clearly expressed for the plagioclases (GOC04 and GOC05; Figure 6c).

In the following, we infer that this rejuvenation within the shear zone is associated with the development of adularia formed from Fe- and K-rich fluids circulating in a network of syntectonic microfractures.

Microprobe analyses show that the granite (GOC04) and the granodiorite (GOC05) are indeed affected by intense fracturing picked out by Fe oxides (Figure 7a), especially the plagioclases. Along these Fe-rich fractures and even if the fractures themselves contain no K (Photo in Figure 7a, GOC05), we observe the development of tiny spots of adularia containing up to 15–17 wt % of K_2O within the plagioclase crystals (Figure 7a and Figure S2 and Table S2 in the supporting information). The size of the adularia micrometric spots is about 50 μm in GOC05 and 30 μm in GOC04 (Figure 7a). The plagioclases from these two samples show evidence of rejuvenation leading at least the primary ages to younger dates at 44.5 ± 1.0, 27.1 ± 0.6, and 27.1 ± 0.6 Ma, respectively. These ages are correlated with the K content and thus probably also with the adularia content. The observed K enrichment within the shear zone, which is associated with younger ages, corresponds here to the synkinematic breakdown of part of the biotite to chlorite, with both Fe and K being dissolved into hydrous fluids circulating along the detachment zone [*Parry and Downey*, 1982].

Away from the shear zone, even though the spots are smaller (10 to 20 μm), the diorite (GOC08) also contains some adularia as well as plagioclases with large patches moderately enriched in potassium (~10 wt %;

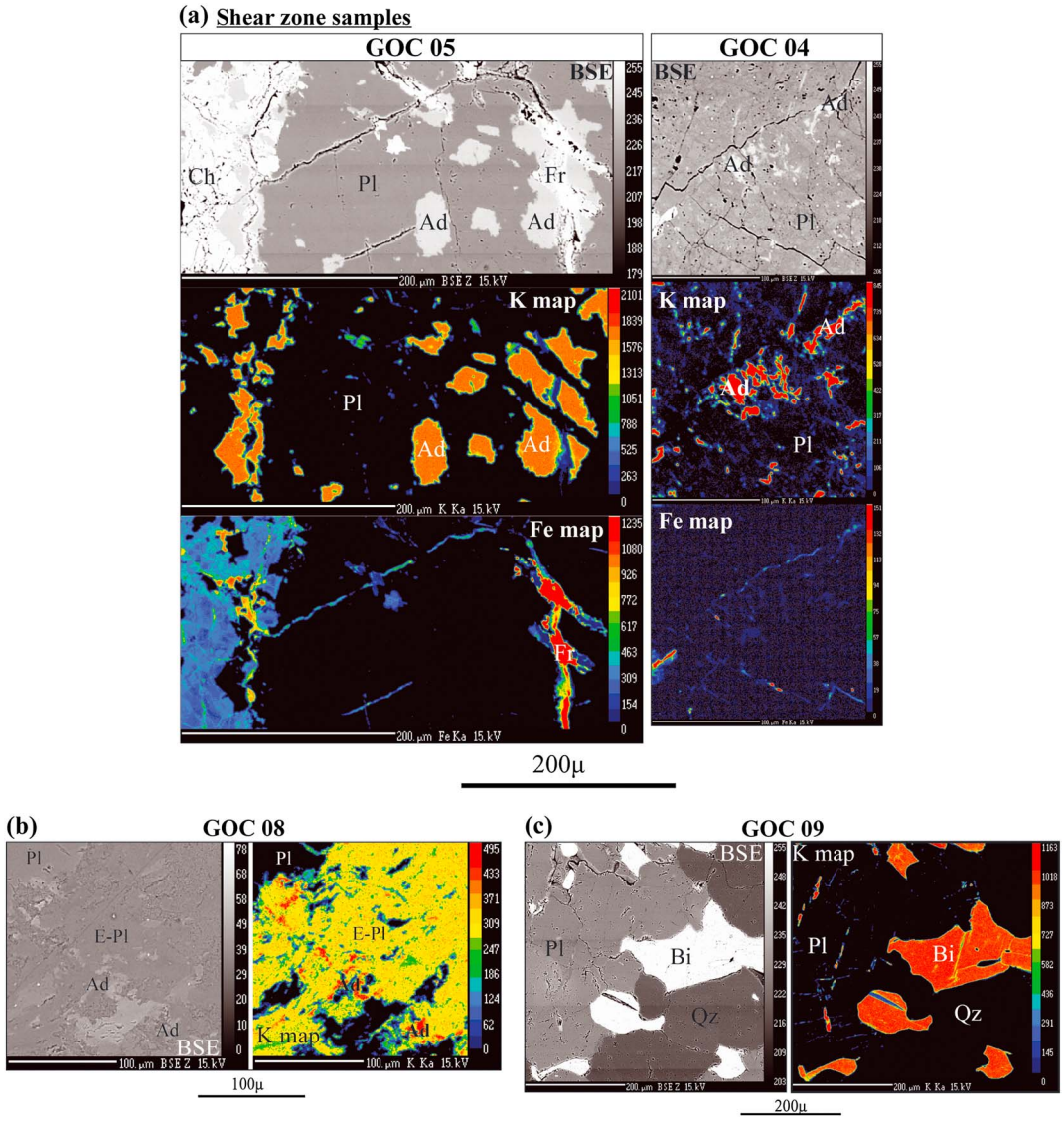

Figure 7. (a) Microprobe analyses with backscattered electron images (BSE) and K and Fe qualitative element maps for samples coming from the shear zone (GOC04 and GOC05). The plagioclases (Pl) show intense fracturing and include little spots of adularia containing up to 15 wt % K_2O. Some of the adularia spots are clearly related to the fracture network. (b) BSE image and K qualitative element maps for GOC08, the feldspars (Pl: plagioclase) show large altered areas moderately enriched in potassium (~10 wt %; E-Pl), in yellow in the K qualitative element map. BSE image and K qualitative element maps for GOC09 (Figure 7b). The biotites are small in size, anhedral habit and show remarkable freshness suggesting they crystallized at a late stage. Contrary to the previous samples, the plagioclases (Pl) show no enrichment in potassium. (Qz: Quartz and Ch: Chlorite).

Figures 7b and S5). This suggests that adularia formed here due to a temperature-controlled intracrystalline diffusion of K at the footwall of the shear zone.

The plagioclase ages obtained from a granitic dike (GOC09) indicate only a slight rejuvenation, and the feldspars display no enrichment in potassium (Figure 7c and Table S4).

The biotites from a granitic dike (GOC09; Figure 7c) have a very small size compared to the general size of minerals in the rock, displaying an anhedral habit and remarkable freshness. Therefore, these biotites are considered as newly crystallized phases with a young age at 18.15 ± 0.43 Ma and not as resulting from a rejuvenation process.

To summarize, the younger ages obtained in the shear zone were rejuvenated as a result of the circulation of potassic fluids, while samples away from the shear zones (GOC8 and GOC9) were affected by a rise in

temperature possibly in connection with the shear zone. 18.15 ± 0.43 Ma determined on newly crystallized biotites for granitic dike (GOC09) possibly marks the major thermal pulse of associated with the extensional tectonics.

Although the top of the shear zone is covered by slope deposits and vegetation, it is highly suggested that this low-dipping decametric extensional shear zone is related to the exhumed footwall deformation of an eastward dipping major detachment fault. As seen hereafter, this interpretation seems to be strengthened by footwall topography and syntectonic deposition within the hanging-wall basin.

3.2. Footwall Morphology of the Sierra La Laguna

The NS trending Sierra La Laguna (SL) culminates at an elevation of more than 2000 m. This massif was considered as the exhumed footwall of the high-angle San José del Cabo fault. This mountain range exhibits several morphologic characteristics. Here we try to find morphologic indices of the detachment fault activity recorded on the topography.

1. It displays asymmetric flanks (Figures 8a and 8c), the eastern flank (bounded by the Los Cabos detachment fault, and the San José del Cabo fault) being wider, while the western flank is steeper (Figure 8c). Furthermore, across-strike topographic profiles along the secondary interfluves of the eastern flank show a convex shape (Figure 8c).
2. The eastern basins are characterized by elongated catchment with a rectilinear parallel pattern of the major streams extending from the fault trace to the main drainage divide (Figure 8a), showing a mean orientation of ~ N103°E ± 3° (Figure 8d) from north to south and are relatively regularly spaced at intervals of 4.5 ± 2.2 km (Figure 8a). This rectilinear pattern is only disrupted by four stream captures in the south (Figure 8a). The second-order streams are not much developed and trend generally orthogonal to the main stream. A dendritic shape of the drainage pattern is solely obtained when the main drainage are affected by stream capture (Figure 8a).
3. The upstream parts of the eastern basins are systematically beheaded, with the valley appearing too wide at its upper end with respect to the present-day catchment surface area (Figure 8b). These beheaded catchments are dry relic valleys which are systematically in continuity with the western basins on both sides of the main drainage divide (Figure 8a).
4. Several faceted spurs up to 400 m high can be observed overhanging the San José del Cabo fault (Figure 8a).

As developed in section 4, we interpret these observations in the geomorphology as the overprint in the footwall topography of a detachment fault and then a high-angle fault activity.

3.3. The Syntectonic San José del Cabo Basin

3.3.1. Age of the Basin

To better constrain the development of the San José del Cabo Basin, we performed four analyses of the cosmogenic nuclides ^{26}Al and ^{10}Be on quartz grains extracted from granitic boulders sampled at the foot of recent and large road cuttings within the Los Barriles formation (Figures 9a and 9b and Table 3). All samples were prepared at the LN^{2}C laboratory, and the analyses were carried out using the French national accelerator mass spectrometry (AMS) facility located at ASTER (CEREGE, France). The ^{26}Al counts measured by the AMS were comparable to results obtained by running blanks and are therefore quoted in Table 3 as maximum values. The resulting ^{26}Al/^{10}Be ratio is consequently very low, with all measured samples yielding values lower than 0.4. By comparing the ^{10}Be concentrations and ^{26}Al/^{10}Be ratios as shown in Figure 9c, we can estimate the age of burial of these detrital samples based on differential decay of these two cosmogenic nuclides after complete shielding from cosmic rays (see *Granger and Muzikar* [2001] for a complete discussion of this approach). Such very low ^{26}Al/^{10}Be ratios, due to the almost complete decay of the previously produced ^{26}Al, indicate that these sediments have been buried for a minimum of 5 Ma (Figure 9c). The position of the representative points on the graph, combined with the fact that the amount of remaining ^{10}Be is higher, also allows us to estimate the initial concentration of cosmogenic nuclides accumulated during erosion processes at the surface, leading to erosion rates of about 50–100 m/Ma.

The very low content of cosmogenic Al in the samples clearly demonstrates that the Los Barriles formation is no younger than 5 Ma (Figure 9c), i.e., early Pliocene at the latest. By establishing that the Los Barriles formation is lower Pliocene (or even older), we need to reconsider significantly the previous age estimates for the southern Baja California sedimentary formations. The Refugio formation is clearly confined to the early Pliocene or even

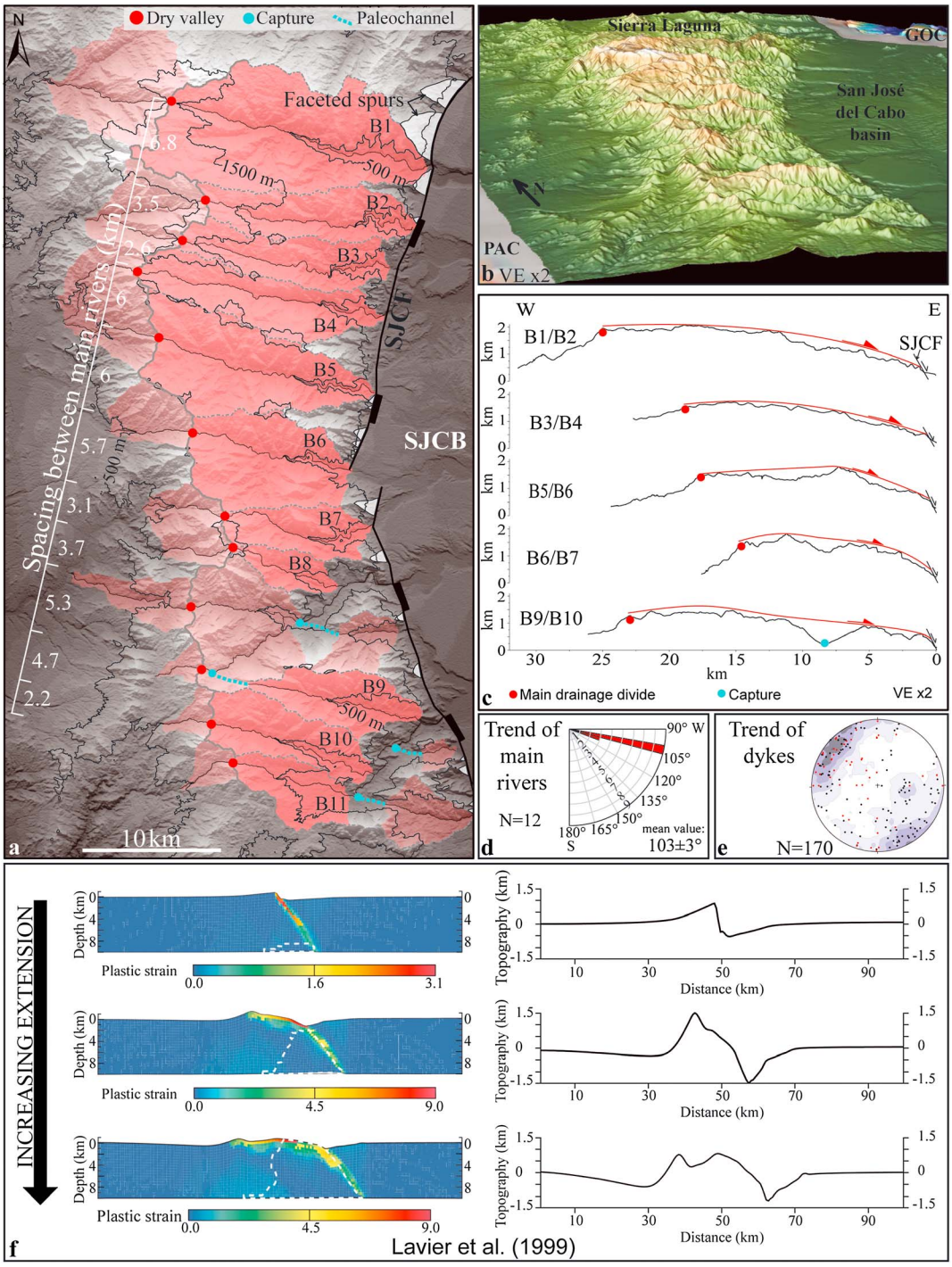

Figure 8. (a) Geomorphologic map of the Sierra la Laguna (SL) showing spacing between the main eastern rivers. The pink catchments represent the inherited drainage network associated with exhumation of the rolling-hinge footwall. Preserved facetted spurs are represented by white triangular shapes, and eroded faceted spurs by light grey triangular shapes. (b) View of a 3-D digital elevation model of the Sierra La Laguna looking toward the east, showing a dry relic valley (Basin *n*°5; location in Figure 8a). Digital elevation model was created using *GeoMapApp* (http://www.GeoMapApp.org). (c) EW trending interfluve profiles, location in Figure 8a. (d) Rose diagram of directional trends of eastern rivers, with average trend of N103°E ± 3° value. (e) Lower hemisphere projection of poles from mafic and acid dikes crosscutting the Sierra La Laguna basement (black squares: present data; red squares: values from *Pérez-Venzor* [2013]) and density contour plots (Kamb method provided by Stereonet program V9.2.0) with 2σ contour interval and 3σ significance level. (f) Model of topography and plastic strain plotted for three steps in the evolution of a detachment fault according to *Lavier et al.* [1999].

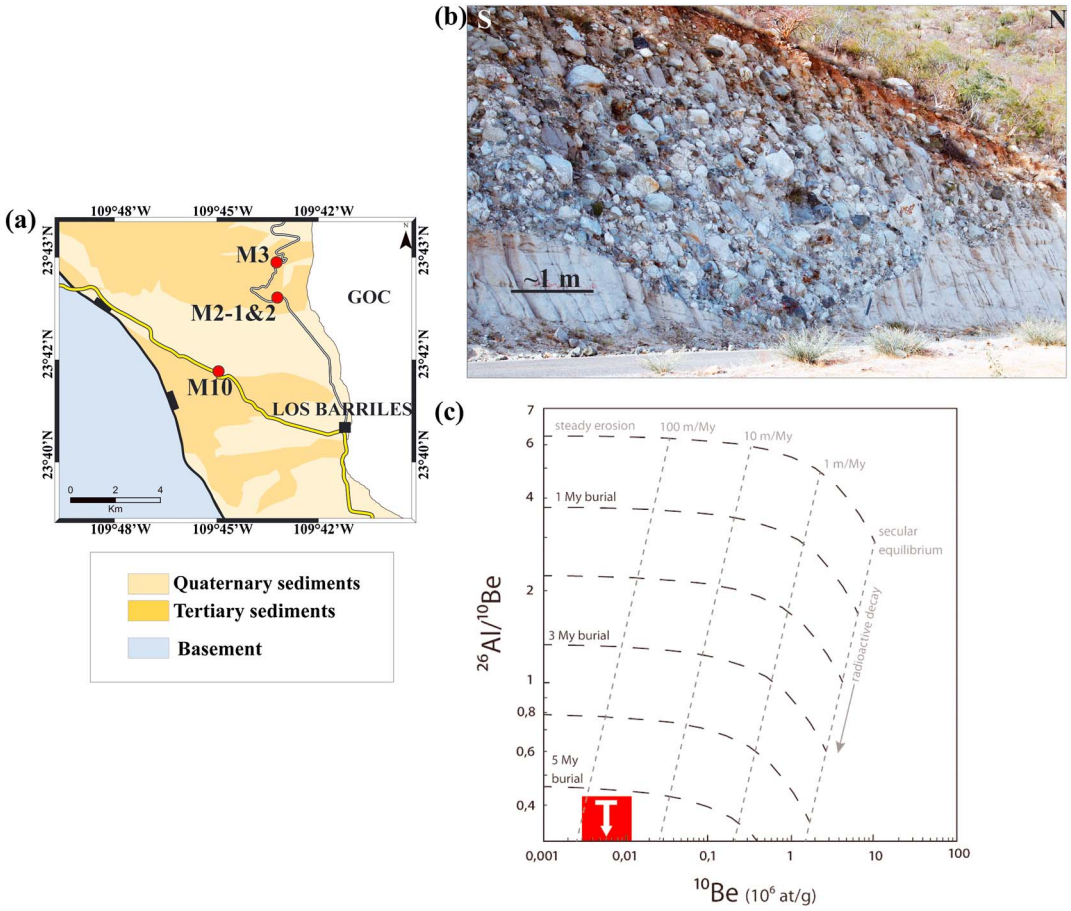

Figure 9. (a) Map of Los Barriles samples of Table 3 (location in Figure 2a). (b) Example of sample site of granitic boulders from Los Barriles formation (M2-1 and M2-2 samples). (c) Burial age plot obtained from concentrations and ratios of cosmogenic nuclides ^{26}Al and ^{10}Be measured in samples of detrital quartz from the Los Barriles formation (calculations from *Granger and Muzikar* [2001]). The very low amount of remaining ^{26}Al (see Table 3) prevents accurate estimation of the ^{26}Al/^{10}Be ratio, so samples are not plotted individually. Samples plot in the red field, which extends down to ^{26}Al/^{10}Be ratios as low as 0.009. Whatever the precision of measurements at such low concentrations, the minimum burial age can be estimated at ~ 5 Ma.

the end Miocene, whereas the Trinidad formation is end Miocene in age at the latest. Therefore, all exposed sedimentary formations, with the exception of the El Chorro formation, appear to be older than 3.6 Ma, so they must predate the lithospheric breakup and the early oceanic spreading at ~3.6 Ma.

Finally, the upper Pleistocene to Holocene El Chorro formation [*Martínez-Gutiérrez and Sethi*, 1997], which unconformably overlies the older strata, corresponds to a postrift deposit.

Table 3. Concentrations of ^{10}Be and ^{26}Al Measured in Shielded Samples of Detrital Quartz From the Los Barriles Formation (Location in Figure 9a)[a]

			^{10}Be		^{26}Al	
Sample	Latitude	Longitude	(at/g)	(±)	(at/g)	^{26}Al/^{10}Be
M2-1	N23°43.845	W109°43.651	6773	709	<771	<0,11
M2-2	N23°43.845	W109°43.651	11205	1134	<4593	<0,41
M3	N23°44.700	W109°43.740	10742	936	<905	<0,09
M10	N23°42.263	W109°44.955	3083	536	<1140	<0,37

[a]Samples were prepared at the LN^{2}C laboratory and measured at the ASTER national AMS facility (CEREGE, France). The total counts acquired for ^{26}Al during AMS measurements ranged from 1 to 2, yielding values comparable to the running blanks. Hence, these results only allow estimation of maximum concentrations. The total initial sample mass used for these measurements was 150 to 250 g of pure quartz.

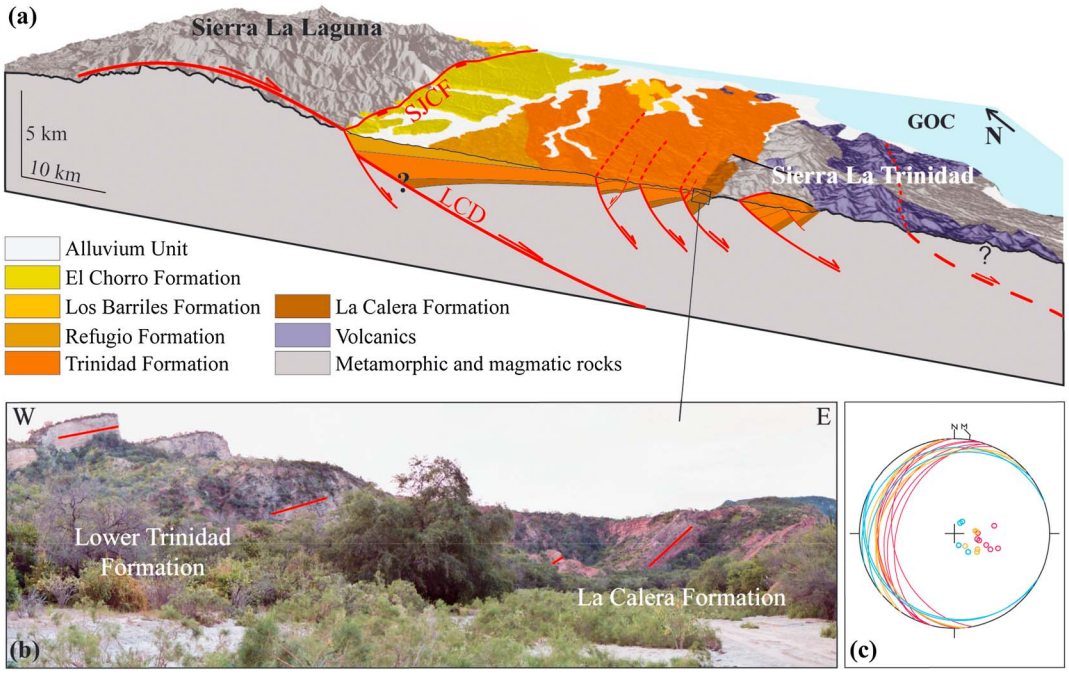

Figure 10. (a) Geological block diagram and cross-section interpretation of the northern part of the San José del Cabo Basin (SJCF: San José del Cabo fault, LCD: Los Cabos detachment; location: white box in Figure 1b; stratigraphy according to *Martínez-Gutiérrez and Sethi* [1997]; sedimentary rock contours from our cartographic analysis and direct observations and from *Martínez-Gutiérrez and Sethi* [1997], and contours of volcanic rocks from *Romero et al.* [2002]); the crustal structure at depth in this area is not known. (b) View of syntectonic sedimentary deposits with fanning bed dip geometry, covering interval from the La Calera formation to the Middle Trinidad formation. (c) Fanning bed dips measured in the same area as Figure 10b (in blue; Lower Trinidad formation; in yellow: upper part of La Calera formation; in red; Lower part of La Calera formation).

3.3.2. Basin Structure

From our cartographic analysis and direct observations, the stratigraphic succession from the middle Miocene La Calera formation to the middle facies of the Trinidad formation is very clearly involved in synsedimentary rift tectonics associated with major normal faults dipping to the east (Figures 10 and 3a–3e). A general fanning bed dip geometry may be observed affecting both formations (Figures 10b and 10c). At the outcrop scale, numerous small-scale faults with normal slip ranging from 1 dm to ~10 m are seen to crosscut both formations. Most of these faults form conjugate sets (Figure 3b). In the La Calera formation up to the Middle Trinidad formation, many of these small-scale normal faults are conjugate and crosscut subhorizontal layers that are sealed by more recent strata and tilted to the west during ongoing extension (Figure 3e). In the claystones of Trinidad formation, many of those faults were associated with local destabilization of the unconsolidated sediments in the hanging walls (slumps; Figure 3e). The amount of stretching within the basin is difficult to estimate as the dip of the major faults is so far unknown.

We used the INVDIR inversion method [*Angelier*, 1990] to determine the reduced stress tensor associated with mechanically compatible fault slip data. This reduced stress tensor [see *Angelier*, 1990] was obtained after untilting the earliest faults (from the La Calera formation to the Middle Trinidad formation) around the averaged strike direction of the strata (Figure 3g). We can compute a minimum stress σ_3 trending N118°E by extracting the stress tensor obtained from the syntectonic deposits of the La Calera formation up to the Middle Trinidad formation (Figure 3g). This stress field probably acted during the middle Miocene to the latest Miocene, i.e., from ~14 to 6 Ma.

We did not observe any strong deformation (i.e., fault-controlled tilting) affecting the Upper Trinidad formation (Figure 3f) within the basin itself, apart from some northern outcrops close the Los Barriles area showing northwestward dipping strata (and probably involved in more recent deformation, see section 4). However, within the San José del Cabo Basin, this formation is cut by a number of minor faults (Figure 3f) recording a stress field with σ_3 trending N088°E (Figure 3h), suggesting an anticlockwise rotation of the horizontal stresses in an extensional regime.

4. Discussion

4.1. The Los Cabos Detachment Fault and Syntectonic Basin

The Los Cabos Block was considered until now as the exhumed footwall of the high-angle San José del Cabo fault. This fault bounds the Sierra La Laguna to the east and trends N010°E in the north and N160°E in the south. It is picked out by spur features that suggest a high-angle fault activity.

However, several arguments contradict this hypothesis. (1) The footwall topography (Figures 8a and 8c) is opposite to that expected for a high-angle normal fault with asymmetric flanks, the eastern flank bounded by the fault being wider, while the western flank is steeper [*Leeder and Jackson*, 1993]. (2) Across-strike topographic profiles along the secondary interfluves of the eastern flank show a convex shape (Figure 8c), a geomorphic characteristics already highlighted on detachment-fault surface in Sulawesi [*Spencer*, 2011]. (3) The remarkably parallel and rectilinear pattern of streams to the east of the main drainage divide (Figure 8a) could indicate recent surface tilting or the presence of a major active normal faults since parallel drainage patterns generally occur as a transitional phase of treillis or dendritic drainage [*Howard*, 1967; *Deffontaines and Chorowicz*, 1991]. But the San José del Cabo fault is currently assumed to be inactive or with a negligible slip rate [*Fletcher and Munguia*, 2000] that makes it difficult to explain the parallel-fault drainage of the Sierra La Laguna. However, such parallel drainage has already been associated to detachment-fault surfaces in New Papua New Guinea [*Miller et al*., 2012]. (4) The N103°E rectilinear and parallel stream pattern (Figures 8a and 8d) cuts obliquely across the fault trace, in particular, in the southern fault segment (Figure 8a).

The dry relic valleys (Figure 8b) in the upper parts of the eastern basins, the continuity and parallelism between the western and eastern basins, as well as the obliquity between the stream trend and the high-angle fault trace seem all controlled by a common parameter. However, this factor is not lithological because the major boundaries between the magmatic basement units have a N-S trend (Figure 2a). The only potential erosional channels in the area are dikes (Figure 8e), but our measurements show, in accordance with the results of *Pérez-Venzor* [2013], that these features trend dominantly NE-SW, i.e., highly oblique to the drainage pattern (Figure 8e). We propose below a structural control of these geomorphic features.

Indeed, we suspect that the parallel geometry of the eastern streams in continuity with the western streams by dry valleys was constrained by regularly spaced corrugations that formed on the convex footwall of a major detachment fault plane, either reflecting the presence of "megamullions" [*Christie et al*., 1998] or folding in a transtensional context [*Seiler et al*., 2010; *Fossen et al*., 2013].

If the river network was contemporaneous to the detachment-fault activity, those dry valleys could be indicative of a drainage reversal during the development of a convex-shaped topography associated with the exhumation of the rolling-hinge footwall [*Lavier et al*., 1999; *Spencer*, 2010] (Figure 8f). The modeling of *Lavier et al*. [1999] indicates that the exhumed detachment fault surface changes from a plane surface dipping toward the hanging wall to a convex shape (Figure 8f). During the first step, the streams on the detachment fault surface must drain only toward the hanging wall, and during the bulging, a new stream network draining toward the opposite sense must develop and piracy the previous stream network by regressive erosion. The dry valleys would correspond to the previous pathway of the first stream network in the hinge of the folded detachment-fault surface.

Considering the estimated dip of the detachment fault plane ($<$20° eastward; Figure 5f) and assuming a 25° C/km thermal gradient, we estimate from fission-track data [*Fletcher et al*., 2000] that rolling hinge deformation of the footwall exhumed at least ~13 km of basement, in accordance with the width of footwall exposure.

The relatively regularly spaced main drainage could be provided a supplementary sign of a structural control even if it is not an argument to a detachment-fault surface since *Hovius* [1996] demonstrates that the regular spacing of the drainage outlets is common during the mountain belt growth. However, it is the combination of a parallel drainage and a regular drainage spacing from upstream to outlet that suggests a drainage network developed on a corrugated detachment fault surface [*Miller et al*., 2012].

As several faceted spurs can be observed overhanging the fault, the particular Los Cabos footwall morphology would therefore result from a superposition of the successive development of upward-convex flexural topography associated with the exhumation of the rolling-hinge footwall due to the observed detachment-fault [*Lavier et al*., 1999; *Spencer*, 2010] (Figures 8c and 8f) with a breakaway zone that is now eroded (Figures 8c and 8f) and late imprint of footwall uplift associated with the San José del Cabo higher-angle fault.

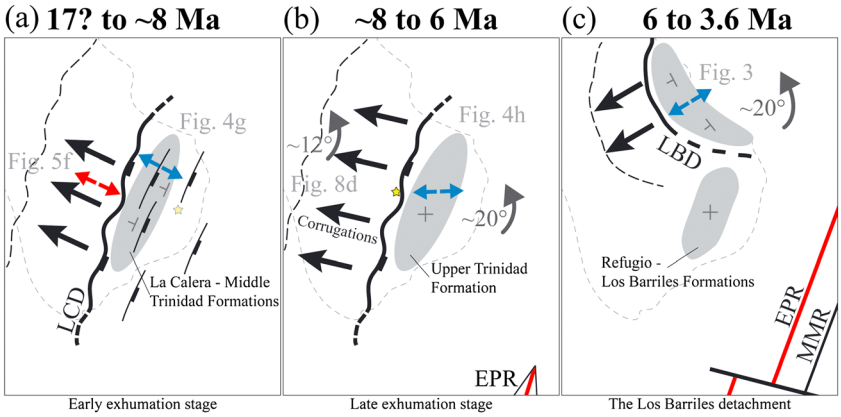

Figure 11. Evolution of the Los Cabos area from ~17 Ma to the breakup stage (3.6 Ma). (a) Early (17?– ~ 8 Ma) and (b) late (~8–6 Ma) exhumation stages of the Los Cabos detachment (LCD) footwall; (c) Later (6–3.6 Ma) Los Barriles detachment (LBD). Red arrows are for stretching directions (Figure 5f). Blue arrows are trends of σ_3 recorded in the La Calera and Lower and Middle Trinidad formations (Figure 11a) (see Figure 3g), in the Upper Trinidad formation (Figure 11b) (see Figure 3h), and in the Los Barriles formation (Figure 11c) [see *Geoffroy and Pronost*, 2010]. Black arrows represent the kinematics at the footwall. The grey dashed lines are the present-day onshore limits. The yellow star is for the displacement of a point located on the detachment plane (buried in Figure 11a and exposed in Figure 11b). EPR: East Pacific Rise and MMR: Maria Magdalena Rise.

4.2. Kinematics and Chronology of the Deformation

We discuss hereafter the detailed kinematics of the Los Cabos area and tentatively replace it in the frame of the GOC opening. We show that the extensional strain field in this area is associated with a continuous anticlockwise rotation of the stretching direction (supposing southern Baja California as fixed) from ~17 to ~3.6 Ma.

4.2.1. Early Exhumation Along the Los Cabos Detachment (Figure 11a)

The motion along the detachment fault has produced ductile to brittle stretching, with synkinematic lineations trending ~ N115°E in the exposed shear zone, developed parallel to the N118°E orientation of σ_3 recorded in the basin during syntectonic sedimentation (Figures 3g, 5f, and 11a).

We can assign a middle Miocene age (~17 to 12 Ma; Figure 11a) for the onset of the Los Cabos detachment considering (1) the age of the earliest observable syntectonic sediments, (2) the apatite and zircon fission track data [*Fletcher et al.*, 2000], and (3) the maximum 17.5 Ma age for the rejuvenation of the basement along the exposed brittle-ductile shear zone (taking into account possible input of allogenic radiogenic Ar within the fluid phase).

In the basin, the earliest sedimentation was controlled by the detachment fault itself and by synthetic faults, expressed notably at the eastern edge of the basin (Figure 10a). The geometry of the basin is hypothetical in its central and western parts, being based on the attitude of bedding from the geological map and from our own dip measurements (Figures 2a and 10a). This geometry suggests a thickening of the basin to the west, which is incompatible with a gravity-derived profile in the northern part of the basin, suggesting a maximum sediment thickness at the center of the basin assuming a constant density for the sediments (from 2 to 2.2 g cm^3) and constant density also for the basement [*Busch et al.*, 2011, Figure 6]. However, these latter authors [*Busch et al.*, 2011] point out that the overall geometry of the basin is asymmetric, highlighting the importance of east facing faults in its structure and excluding the San José del Cabo fault as a major synsedimentary structure during the Mio-Pliocene, in contrast with previous considerations. Although we agree with that, we consider that the inversion of gravity data in the southern Baja California basins should take better account of the footwall-related sedimentary facies as described by *Martínez-Gutiérrez and Sethi* [1997]. These authors stressed that conglomeratic formations with abundant submetric to metric basement boulders are common along the basin boundary faults, even at distance from them. This could indicate that large lateral density gradients are to be expected within these basins. For example, 50% of boulders of density $>$2.6 g cm^3 contained in a matrix of density 2.2 g cm^3 gives an average conglomerate density of $>$2.4 g cm^3, which would significantly thicken the basin along the faults. Alternatively, although our reconstruction from Figure 10a fits with the exposed geology, it does not take into account possible concealed

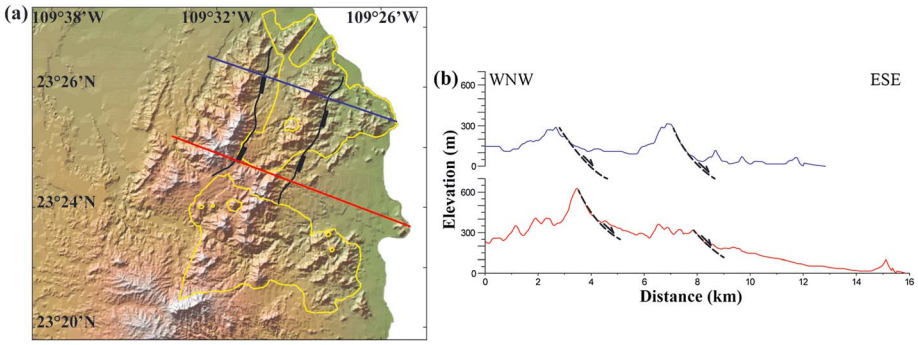

Figure 12. (a) Shaded relief map of the Sierra La Trinidad and mapping of probable synthetic detachment faults associated with the Los Cabos detachment (for location: see Figure 1b). The dotted yellow lines correspond to contours of volcanic rocks [*Romero et al*., 2002]. Digital elevation model and profiles were created using *GeoMapApp* (http://www.GeoMapApp.org). (b) Topographic profiles located in Figure 12a. Dashed lines indicate probable fault planes.

normal faults dipping to the east at the western edge of the basin and sealed by the Trinidad formation and later sedimentary deposits.

To the east of the basin, the upper plate Trinidad basement block is probably itself dissected eastward by an array of at least two large normal faults dipping ESE, considering both the topography and the location of outcropping Miocene-related volcanics (Figures 10a, 12**,** and 13).

4.2.2. Late Exhumation Along the Detachment Fault (Figure 11b)

The detachment is thought to have been inactive from the end Miocene (Figure 11b), just before the development of the Los Barriles detachment and the onset of the earliest oceanic crust accretion in the nearby EPR propagator segment (Figures 1 and 11c). These ages are in very good agreement with major exhumation of the eastern part of the Sierra La Laguna during the middle to early Pliocene, as inferred by *Fletcher at al*. [2000] from apatite and zircon fission track data.

We infer that a slight (~10°) anticlockwise rotation in the strain field occurred during the late footwall exhumation as expressed both in the sole of the detachment (which is made up of the Sierra La Laguna basement) and in the hanging-wall basin.

We note indeed a ~12° anticlockwise discrepancy between the N103°E trending rivers equated with corrugations (Figure 8d) and the initial N115°E kinematic trend (Figure 5f). These corrugations on detachments can be interpreted as megamullions formed by frictional shear or, alternatively, by basement folding in a transtensional context [*Seiler et al*., 2010; *Fossen et al*., 2013]. In the latter case, the corrugation could either be parallel to the instantaneous *X* axis (maximum stretching direction) or the initial hinge lines, which were formed at 90° to the shear plane and passively rotated during increasing transtension [*Fossen et al*., 2013]. Although we do not observe any folding in the basin itself, and even if short-wavelength folding of an upper/middle crustal basement would imply unexpected high thermal gradients, we should not completely rule out this hypothesis of a slight strike-slip shear component during extension.

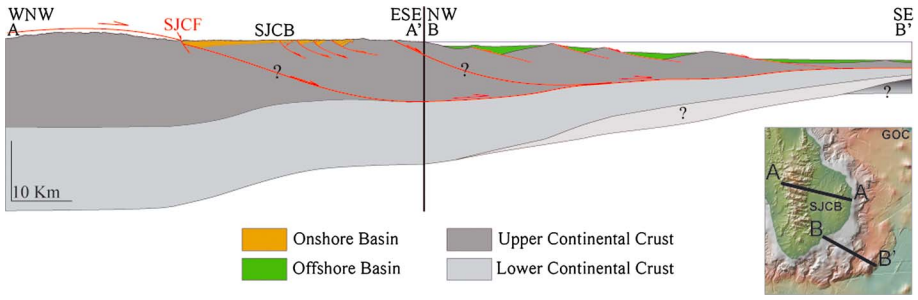

Figure 13. Composite AA' and BB' (see inset and Figure 1b) cross section of the Los Cabos margin. The offshore faults and basins location after *Páramo et al*. [2008]; crustal structures modified from *Páramo et al*. [2008]. The crust thins from 28 km in continental crust to 6.7 km in oceanic crust, and the thinned continental crust occupies a 75 km wide zone.

However, synsedimentation faulting within the basin shows also a ~20° anticlockwise rotation of the minimum stress associated with the deposition of the Upper Trinidad syntectonic formation (compare Figures 3g and 3h). We are thus prone to conclude that the inferred N103°E corrugations in the detachment footwall (Figure 8d) represent the tectonic imprint of the latest stages of the footwall exhumation in the frame of a general anticlockwise rotation of the stretching direction.

4.2.3. Final Exhumation: The Los Barriles Detachment (Figure 11c)

Contrary to what is observed in the Los Cabos Basin, the Refugio and Los Barriles formations which postdate the Trinidad are clearly involved in detachment-type tectonics in the Los Barriles area, to the north of the San José del Cabo Basin (Figures 1b and 4) [*Geoffroy et al*., 2009; *Geoffroy and Pronost*, 2010; *Masini et al*., 2010]. The related detachment fault bordering the Los Barriles Basin (LBB in Figures 1b and 11c) was initially mapped as the northwestward continuation of the San José del Cabo Fault [*Fletcher and Munguia*, 2000; *Busch et al*., 2011] in clear contradiction with detailed mapping [*Romero et al*., 2002] as well as field observations. The kinematic vector of the N160°E trending Los Barriles detachment fault is N070°E ± 20° thus anticlockwise rotated compared to the previous N088°E to N118°E vector inferred from the San José del Cabo Basin.

4.2.4. Latest Tectonics

From this stage onward, the high-angle San José del Cabo fault (as well as a number of other faults in the area such as San Juan de Los Planes fault, Figure 1b) crosscuts the Los Cabos area detachment fault, apparently accommodating only minor extension in the ~ N090 to N120°E trend. This renewed E-W to NW-SE extension, coeval with the El Chorro deposition (Figure 10a), is of regional distribution [*Coletta and Angelier*, 1983; *Umhoefer et al*, 2002].

4.3. Geodynamic Interpretation (Figure 14)

The geometry and kinematics of the postulated detachment, as well as development of the coeval basin, are clearly related in time and space to the continental strain field associated with the NE ward propagation of the EPR axis during the Miocene [*Curray et al*., 1982; *Lonsdale*, 1991, 1989] (Figure 13 with location in Figure 1b). The Los Cabos detachment fault is associated with continental margin necking as imaged by *Páramo et al*. [2008] farther south from seismic refraction and gravity survey data (Figure 13). We propose a synthesis of the available and new data in Figure 13. The Los Cabos detachment would represent continentward crustal necking related to a seaward dipping detachment fault on the passive margin, as proposed in recent models of nonmagmatic continental breakup [*Manatschal*, 2004; *Mohn et al*., 2010; *Unternehr et al*., 2010]. We also suggest that this fault could root along the brittle/ductile interface at depth [*Whitney et al*., 2013] (Figure 13). This hypothesis is in agreement with the NW-SE extension affecting basins on the Alarcón spreading corridor subsequent to approximately 14–12 Ma [*Sutherland et al*., 2012]. Because the Upper Trinidad Formation seems to postdate extensional tectonics within the Los Cabos basin, we tentatively correlate this formation with the early Pliocene continental breakup and earliest thermal relaxation of the margin lithosphere in this area.

On the other hand, there is abundant evidence that NE-SW to ENE-WSW extension occurred during the middle to late Miocene across most of the future GOC in a trend nearly orthogonal to the Comundu volcanic arc [*Angelier et al*., 1981; *Stock and Hodges*, 1989; *Zanchi*, 1994].

Therefore, we may tentatively infer the following tectonic evolution in southern Baja California (Figure 14):

1. During an early late Miocene stage, from 14 to 6 Ma, two strain fields coexisted in southern Baja California when the EPR ridge propagator was approaching the Cabo-PV area: NE-SW to ENE-WSW extension across most of the Peninsula (acting since the Miocene) and NW-SE (N118°E) in the Cabo-PV and Alarcon areas (Figure 13a); the NW-SE extension would have been driven by tensional tectonic stresses associated with the tip of the EPR propagator, whereas the NE-SW to ENE-WSW extension was probably driven by slab-related deep processes [*Martín et al*., 2000] and/or by gravity collapse of the Comundu arc inducing lower crustal flow [e.g., *Persaud et al*., 2007]. It is probable that at this stage, the southern prolongation of the San Andreas dextral shear zone (partly?) jumped from the San Benito and Tosco-Abreojos faults (Figures 1a and 14a) and became localized toward the center of the GOC, adopting an en echelon pattern corresponding to a purely dextral shear zone [*Bennett et al*., 2013] (Figure 14a).
2. Probably ~1–2 Ma before definitive breakup in the Cabo-Puerto Vallarta area (i.e., at about ~6 Ma), the NW-SE to E-W continental extension ceased and displacement was mainly transferred into the breakup

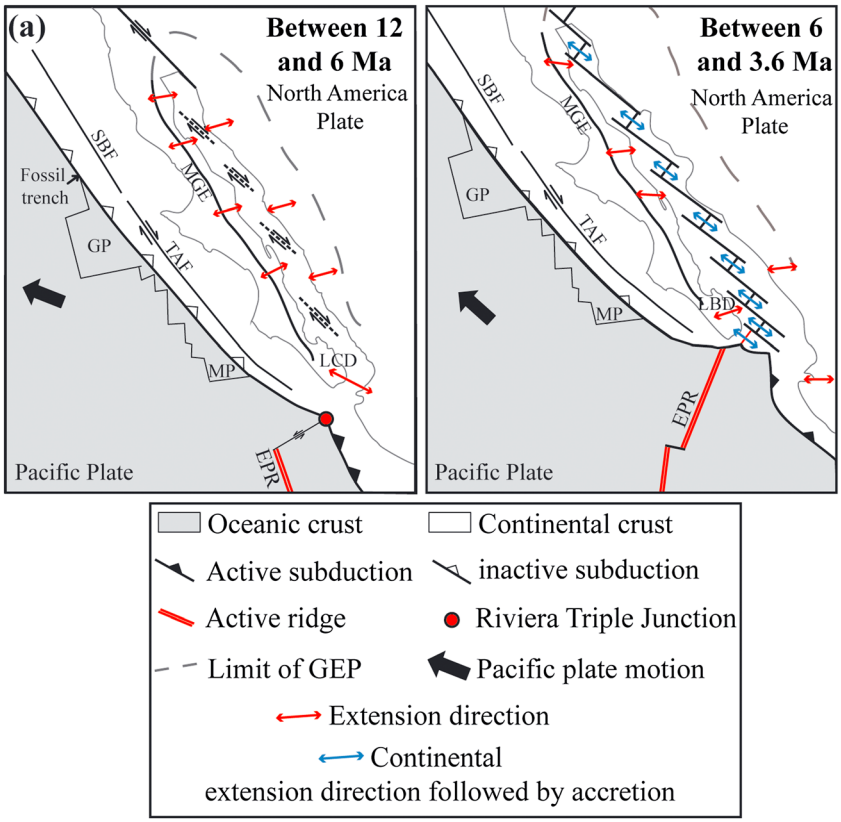

Figure 14. Proposed tectonic evolution with extension directions recorded along the structures of the Gulf of California during continental extension according to our data and the results of *Angelier et al.* [1981], *Bennett et al.* [2013], *Gans* [1997], *Geoffroy and Pronost* [2010], *Henry and Aranda-Gomez* [2000], *Lee et al.* [1996], *Oskin and Stock* [2003a], *Stock and Hodges* [1989], and *Zanchi* [1994]. Plate motion vectors are from *Atwater and Stock* [1998]. Oceanic structures are from *Lonsdale* [1989, 1995]. GEP and MGE are modified from *Axen* [1995]. Onshore limits are modified from *Fletcher et al.* [2007] and *Drake* [2005]. (a) Stage from ~12 Ma and 6 Ma; (b) stage from 6 Ma. GEP: Gulf Extensional Province, MGE: Main Gulf Escarpment, EPR: East Pacific Rise, MP: Magdalena Plate, GP: Guadalupe Plate, LCD: Los Cabos Detachment, LBD: Los Barriles detachment, TAF: Tosco-Abreojos fault, and SBF: San Bonito fault.

area, as indicated by the late-rift attitude of the Upper Trinidad formation. Within the central GOC, continental extension followed by early accretion seems parallel to the regional NW-SE plate motion vector [*Plattner et al.*, 2009], as suggested by the observed pattern of normal faults trending NNE-SSW, accommodating the pull-apart breakup of the central part of the GOC (Figure 14b) [*Lonsdale*, 1989; *Umheofer*, 2011; *Sutherland et al.*, 2012]. At the same period, along the GOC onshore margins, the inherited Gulf-parallel faults continued to act as pure dip-slip faults and dextral oblique-slip faults accommodating an ENE-WSW trending extension.

This GOC normal extension turned finally to NW-SE [*Angelier et al.*, 1981, *Colletta and Angelier* 1983; *Geoffroy and Pronost*, 2010; *Umhoefer et al.*, 2007]. The development of some newly formed N-S to NE-SW high-angle normal faults [*Umhoefer et al.*, 2014], including possibly the San José del Cabo fault, is consistent with this latest evolution. However this late NW-SE extension is weak and probably transient since the present-day stress field indicated by earthquakes along the margin is more consistent with NE-SW extension [*Munguía et al.*, 2006]. This active tectonics could be connected to lateral displacement currently observed in the western part of Baja California along the Tosco-Abreojos faults [*Michaud et al.*, 2004], suggesting some strain partitioning in this area.

The general pattern, with extension parallel to the kinematic vector in the central GOC area, but oblique along rift-parallel normal faults at the borders of the Gulf, is in very good agreement with the recent model of oblique rifting proposed by *Philippon et al.* [2015]. In this model, this particular pattern would arise in relation with the deformation of a linear belt of weak crust trending oblique to the kinematic vector. This weak crust would here represent the thickened arc-related Oligo-Miocene crust of the GOC.

5. Conclusions

1. A crustal-scale detachment along the Sierra La Laguna in southern Baja California, unrecognized until now, exhibits a >10 m wide ductile to cataclastic shear zone dipping ~20° to the SE. The ~ E-W trending regularly spaced drainage pattern of the convex detachment footwall is best interpreted as representing megamullions. The continuity between the eastern and western basins away from the dry relic valleys in the detachment footwall could suggest an upward-convex flexural doming of the detachment fault plane with a breakaway zone that has been eroded. The present morphology of the Sierra La Laguna would represent the fossilized and partly eroded exhumed footwall of the Los Cabos detachment fault which was inactive from ~6 Ma.
2. At the hanging wall of the detachment fault, the stratigraphic succession from the middle-Miocene La Calera formation to the middle member of the Trinidad formation in the San Jose del Cabo Basin is clearly involved in synsedimentary rift tectonics, which is kinematically coherent with the motion vectors along the detachment fault. In addition, the age of synsedimentary extension, constrained by cosmogenic isotopes, is globally consistent with the ages inferred from K-Ar dating along the shear zone itself (~17 Ma for the maximum age of rejuvenation from K/Ar ages in the basement) and also from fission track data [*Fletcher et al*., 2000]. A minimum stress σ_3 vector trending N118°E anticlockwise rotating lately to N088°E is obtained in the basin from the inversion of fault slip data derived from synsedimentary normal faults.
3. To the north of the Sierra La Laguna, along the shore of the NW-SE trending GOC, another synsedimentary detachment structure crosscuts and postdates the Los Cabos detachment fault [*Geoffroy and Pronost*, 2010]. The Los Barriles detachment was active during the deposition of the Refugio and Los Barriles formations, which we show here to be no younger than 5 Ma. The kinematic vector associated with this detachment trends N070°E ± 20° outlining the anticlockwise rotation of the stretching directions during a ~12 Ma period in southern Baja California. The San José del Cabo fault and a number of minor faults in the nearby Quaternary basins of southern Baja California record a late extension in the E-W to NW-SE trend. These faults accommodate a minor deformation compared to the deformation associated with detachment structures.

The pattern of extension on the southern Baja California margin thus appears to be much more complex than initially suggested from studies focused on high-angle recent to active faults [*Busch et al*., 2011; *Fletcher and Munguia*, 2000; *Fletcher et al*., 2000; *Umhoefer et al*., 2014]. To the south of the area, an overlapping of detachment faults and basins is observed with different kinematics and ages. By integrating the data at the scale of the GOC, it appears that southern Baja California was greatly influenced by the northeastward EPR propagation during the Miocene-Pliocene. The related strain field should not be confused with more recent late Pliocene-Quaternary tectonics. Apart from this strain field that was localized in time and space, the overall deformation of the GOC and its margins since the Miocene seems to be best explained by the existence of a central weak zone (corresponding to the GOC). This latter domain is highly oblique to the plate motion vector, with faults showing contrasted geometries in the center of the weak zone and along its borders [*Philippon et al*., 2015].

Acknowledgments
This project is supported by the "Action Marges" program (CNRS-INSU, TOTAL, IFREMER, BRGM). Céline Liorzou and Jessica Langlade are warmly thanked for their technical assistance in geochemical and microprobe analyses, respectively. We thank Luc Lavier for permission to display the figure of his model. We are also grateful to Gary Axen and the anonymous reviewers for their constructive comments and suggestions that have contributed to improve this paper. Michael Carpenter postedited the English style and grammar. The data for this paper are available by contacting the corresponding author.

References

Angelier, J. (1990), Inversion of field data in fault tectonics to obtain the regional stress—III, A new rapid direct inversion method by analytical means, *Geophys. J. Int.*, *103*(2), 363–376, doi:10.1111/j.1365-246X.1990.tb01777.x.

Angelier, J., B. Colletta, J. Chorowicz, L. Ortlieb, and C. Rangin (1981), Fault tectonics of the Baja California Peninsula and the opening of the Sea of Cortez, Mexico, *J. Struct. Geol.*, *3*(4), 347–357, doi:10.1016/0191-8141(81)90035-3.

Arreguín-Rodríguez, G. D. J., and T. Schwennicke (2013), Estratigrafía de la margen occidental de la cuenca San José del Cabo, Baja California Sur, *Boletín de la Sociedad Geológica Mexicana*, *65*(3), 481–496.

Atwater, T., and J. Stock (1998), Pacific-North America plate tectonics of the Neogene southwestern United States, *Int. Geol. Rev.*, *40*(5), 375–402.

Autin, J., N. Bellahsen, L. Husson, M.-O. Beslier, S. Leroy, and E. d' Acremont (2010a), Analog models of oblique rifting in a cold lithosphere, *Tectonics*, *29*, TC6016, doi:10.1029/2010TC002671.

Autin, J., N. Bellahsen, S. Leroy, L. Husson, M.-O. Beslier, and E. d' Acremont (2013), The role of structural inheritance in oblique rifting: Insights from analogue models and application to the Gulf of Aden, *Tectonophysics*, *607*, 51–64.

Axen, G. (1995), Extensional segmentation of the Main Gulf Escarpment, Mexico and United States, *Geology*, *23*, 515–518, doi:10.1130/0091-7613(1995)023<0515:ESOTMG>2.3.CO;2.

Bellahsen, N., L. Husson, J. Autin, S. Leroy, and E. d'Acremont (2013a), The effect of thermal weakening and buoyancy forces on rift localization: Field evidences from the Gulf of Aden oblique rifting, *Tectonophysics*, *607*, 80–97, doi:10.1016/j.tecto.2013.05.042.

Bellon, H., N. Quoc Buü, J. Chaumont, and J. C. Philippet (1981), Implantation ionique d'argon dans une cible support: Application au traçage isotopique de l'argon contenu dans les minéraux et les roches, *C. R. Acad. Sci. Paris*, *292*, 977–980.

Bennett, S. E. K., M. E. Oskin, and A. Iriondo (2013), Transtensional rifting in the proto–Gulf of California near Bahía Kino, Sonora, México, *GSA Bull.*, *125*, 1752–1782, doi:10.1130/B30676.1.

Bryan, S. E., T. Orozco-Esquivel, L. Ferrari, and M. López-Martínez (2014), Pulling apart the Mid to Late Cenozoic magmatic record of the Gulf of California: Is there a Comondú Arc?, *Geol. Soc. London, Spec. Publ.*, *385*(1), 389–407.
Brune, S. (2014), Evolution of stress and fault patterns in oblique rift systems: 3-D numerical lithospheric-scale experiments from rift to breakup, *Geochem. Geophys. Geosyst.*, *15*, 3392–3415, doi:10.1002/2014GC005446.
Busch, M. M., J. R. Arrowsmith, P. J. Umhoefer, J. A. Coyan, S. J. Maloney, and G. M. Gutiérrez (2011), Geometry and evolution of rift-margin, normal-fault–bounded basins from gravity and geology, La Paz–Los Cabos region, Baja California Sur, Mexico, *Lithosphere*, *3*, 110–127, doi:10.1130/L113.1.
Christie, D. M., B. P. West, D. G. Pyle, and B. B. Hanan (1998), Chaotic topography, mantle flow and mantle migration in the Australian-Antarctic discordance, *Nature*, *394*(6694), 637–644, doi:10.1038/29226.
Colletta, B., and J. Angelier (1983), Tectonique cassante du nord-ouest mexicain et ouverture du Golfe de Californie, *Bull. Cent. Rech. Explor. Prod. Elf-Aquitaine*, *7*, 433–441.
Cox, A., and G. B. Dalrymple (1967), Statistical analysis of geomagnetic reversal data and the precision of potassium-argon dating, *J. Geophys. Res.*, *72*(10), 2603–2614, doi:10.1029/JZ072i010p02603.
Curray, J. R., D. G. Moore, K. Kelts, and G. Einsele (1982), Tectonics and geological history of the passive continental-margin at the tip of Baja California, Initial Reports of the Deep Sea Drilling Project, 64(OCT), 1089.
Deffontaines, B., and J. Chorowicz (1991), Principles of drainage basin analysis from multisource data: Application to the structural analysis of the Zaire Basin, *Tectonophysics*, *194*(3), 237–263.
DeMets, C. (1995), A reappraisal of seafloor spreading lineations in the Gulf of California: Implications for the transfer of Baja California to the Pacific Plate and estimates of Pacific-North America Motion, *Geophys. Res. Lett.*, *22*(24), 3545–3548, doi:10.1029/95GL03323.
Drake, W. R. (2005), Structural analysis, stratigraphy, and geochronology of the San José Island accommodation zone, MS thesis, Northern Arizona Univ., Baja California Sur, Mexico.
Ferrari, L., M. Valencia-Moreno, and S. Bryan (2007), Magmatism and tectonics of the Sierra Madre Occidental and its relation with the evolution of the western margin of North America, in *Geology of México: Celebrating the Centenary of the Geological Society of México*, edited by S. A. Alaniz-Álvarez and Á. F. Nieto-Samaniego, *Geol. Soc. Am. Spec. Pap.*, *422*, 1–39.
Fletcher, J. M., and L. Munguia (2000), Active continental rifting in southern Baja California, Mexico: Implications for plate motion partitioning and the transition to seafloor spreading in the Gulf of California, *Tectonics*, *19*(6), 1107–1123, doi:10.1029/1999TC001131.
Fletcher, J. M., B. P. Kohn, D. A. Foster, and A. J. Gleadow (2000), Heterogeneous Neogene cooling and exhumation of the Los Cabos block, southern Baja California: Evidence from fission-track thermochronology, *Geology*, *28*(2), 107–110.
Fletcher, J. M., M. Grove, D. Kimbrough, O. Lovera, and G. E. Gehrels (2007), Ridge-trench interactions and the Neogene tectonic evolution of the Magdalena shelf and southern Gulf of California: Insights from detrital zircon U-Pb ages from the Magdalena fan and adjacent areas, *Geol. Soc. Am. Bull.*, *119*, 1313–1336, doi:10.1130/B26067.1.
Fournier, M., N. Bellahsen, O. Fabbri, and Y. Gunnell (2004), Oblique rifting and segmentation of the NE Gulf of Aden passive margin, *Geochem. Geophys. Geosyst.*, *5*, Q11005, doi:10.1029/2004GC000731.
Fossen, H., C. Teyssier, and D. L. Whitney (2013), Transtensional folding, *J. Struct. Geol.*, *56*, 89–102, doi:10.1016/j.jsg.2013.09.004.
Gans, P. B. (1997), Large-magnitude Oligo-Miocene extension in southern Sonora: Implications for the tectonic evolution of northwest Mexico, *Tectonics*, *16*(3), 388–408, doi:10.1029/97TC00496.
Gastil, R. G., R. P. Phillips, and E. C. Allison (1975), Reconnaissance geology of the state of Baja California, *Geol. Soc. Am. Mem.*, *140*, 1–201, doi:10.1130/MEM140-p1.
Geoffroy, L., and J. Pronost (2010), Late Pliocene to Early Quaternary extensional detachment in the La Paz–El Cabo area (Baja California Sur, Mexico): Implications on the opening of the Gulf of California and the mechanics of oblique rifting, *Terra Nova*, *22*, 64–69.
Geoffroy, L., E. Masini, C. Robin, and P. Strzerzynski (2009), Detachment tectonics and hangingwall sedimentation: The Late Pliocene-Holocene Los Barriles Basin, Baja California Sur (Mexico): AGU Fall Meeting Abstracts, v. 1, p. 1828.
Granger, D. E., and P. F. Muzikar (2001), Dating sediment burial with in situ-produced cosmogenic nuclides: Theory, techniques, and limitations, *Earth Planet. Sci. Lett.*, *188*(1), 269–281.
Hausback, D. E. (1984), Cenozoic volcanic and tectonic evolution of Baja California Sur, Mexico, in *Geology of the Baja California Peninsula: Bakersfield, California, Pacific Section*, edited by V. A. Frizzell, Society of Economic Paleontologists and Mineralogists, pp. 219–236.
Henry, C. D., and J. J. Aranda-Gomez (2000), Plate interactions control middle–late Miocene, proto-Gulf and Basin and Range extension in the southern Basin and Range, *Tectonophysics*, *318*(1), 1–26, doi:10.1016/S0040-1951(99)00304-2.
Hovius, N. (1996), Regular spacing of drainage outlets from linear mountain belts, *Basin Res.*, *8*, 29–44.
Howard, A. D. (1967), Drainage analysis in geologic interpretation: A summation, *AAPG Bull.*, *51*(11), 2246–2259.
Karig, D. E., and W. Jensky (1972), The proto-gulf of California, *Earth Planet. Sci. Lett.*, *17*(1), 169–174, doi:10.1016/0012-821X(72)90272-5.
Lavier, L. L., W. R. Buck, and A. N. Poliakov (1999), Self-consistent rolling-hinge model for the evolution of large-offset low-angle normal faults, *Geology*, *27*(12), 1127–1130.
Leeder, M. R., and J. A. Jackson (1993), The interaction between normal faulting and drainage in active extensional basins, with examples from the western United States and central Greece, *Basin Res.*, *5*(2), 79–102.
Lee, J., M. M. Miller, R. Crippen, B. Hacker, and J. L. Vazquez (1996), Middle Miocene extension in the Gulf extensional province, Baja California: Evidence from the southern Sierra Juarez, *Geol. Soc. Am. Bull.*, *108*(5), 505–525, doi:10.1130/0016-7606(1996)108<0505:MMEITG>2.3.CO;2.
Leroy, S., et al. (2012), From rifting to oceanic spreading in the Gulf of Aden: A synthesis, *Arab J. Geosci.*, *5*, 859–901, doi:10.1007/s12517-011-0475-4.
Lewis, C. J., and J. M. Stock (1998), Paleomagnetic evidence of localized vertical axis rotation during Neogene extension, Sierra San Fermin, northeastern Baja California, Mexico, *J. Geophys. Res.*, *103*(B2), 2455–2470.
Lewis, J. L., S. M. Day, H. Magistrale, R. R. Castro, L. Astiz, C. Rebollar, J. Eakins, F. L. Vernon, and J. N. Brune (2001), Crustal thickness of the peninsular ranges and gulf extensional province in the Californias, *J. Geophys. Res.*, *106*(B7), 13,599–13,611.
Liu, M. (2001), Cenozoic extension and magmatism in the North American Cordillera: The role of gravitational collapse, *Tectonophysics*, *342*(3), 407–433, doi:10.1016/S0040-1951(01)00173-1.
Lizarralde, D., G. J. Axen, H. E. Brown, J. M. Fletcher, A. González-Fernández, A. J. Harding, W. S. Holbrook, G. M. Kent, P. Paramo, and F. Sutherland (2007), Variation in styles of rifting in the Gulf of California, *Nature*, *448*, 466–469, doi:10.1038/nature06035.
Lonsdale, P. (1989), Geology and tectonic history of the Gulf of California, in *The Eastern Pacific Ocean and Hawaii*, vol. N, edited by E. L. Winterer et al., pp. 499–521, Geol. Soc. of Am., Boulder.
Lonsdale, P. (1991), Structural patterns of the Pacific floor offshore of peninsular California, in *The Gulf and the Peninsular Province of the Californias*, edited by J. P. Dauphin and B. R. T. Simoneit, *Mem. Am. Assoc. Pet. Geol.*, *47*, 87–125.
Lonsdale, P. (1995), Segmentation and disruption of the East Pacific Rise in the mouth of the Gulf of California, *Mar. Geophys. Res.*, *17*(4), 323–359.

Lyle, M., and G. E. Ness (1991), The opening of the southern Gulf of California, in *The Gulf and the Peninsular Province of the Californias*, edited by J. P. Dauphin and B. R. T. Simoneit, *Mem. Am. Assoc. Pet. Geol.*, *47*, 403–423.
Manatschal, G. (2004), New models for evolution of magma-poor rifted margins based on a review of data and concepts from West Iberia and the Alps, *Int. J. Earth Sci.*, *93*, 432–466.
Martínez-Gutiérrez, G., and P. S. Sethi (1997), Miocene-Pleistocene sediments within the San José del Cabo Basin, Baja California Sur, Mexico, in *Pliocene Carbonates and Related Facies Flanking the Gulf of California*, edited by M. E. Johnson and J. Ledesma-Vázquez, *Geol. Soc. Am. Spec. Pap.*, *318*, 141–166.
Martín, A.,. J., M. Fletcher, M. López-Martínez, and R. Mendoza-Borunda (2000), Waning Miocene subduction and arc volcanism in Baja California: The San Luis Gonzaga volcanic field, *Tectonophysics*, *318*(1–4), 27–51, doi:10.1016/S0040-1951(99)00305-4.
Masini, E., C. Robin, L. Geoffroy, and P. Strzerzynski (2010), The supra-detachment tectono-sedimentary record of rifted margins: The example of the Los Barriles Basin, SE Baja California Sur (resumen) en EGU General Assembly Conference Abstracts, 12, EGU2010-12049.
McCloy, C. (1984), Stratigraphy and depositional history of the San José del Cabo trough, Baja California Sur, Mexico, in *Geology of the Baja California Peninsula*, vol. 39, edited by V. A. Frizzell, pp. 253–265, Pac. Sect. Soc. Of Econ. Paleontol. and Mineral, Calif.
McTeague, M. S., P. J. Umhoefer, T. Schwennicke, and J. C. Ingle (2005), Sedimentary record of Miocene rifting along the eastern side of the San Jose del Cabo Basin, Baja California Sur, Mexico: Critical early evidence of the proto Gulf of California. In 2005 Salt Lake City Annual Meeting.
McTeague, M. S., P. J. Umhoefer, T. Schwennicke, J. C. Ingle, and M. Cortes Martinez (2006), Evolution of the east-central San Jose del Cabo Basin, Baja California Sur, Mexico, in AGU Fall Meeting Abstracts (Vol. 1, p. 1611).
Michaud, F., M. Sosson, J. Y. Royer, A. Chabert, J. Bourgois, T. Calmus, and B. Pontoise (2004), Motion partitioning between the Pacific plate, Baja California and the North America plate: The Tosco-Abreojos fault revisited, *Geophys. Res. Lett.*, *31* L08604, doi:10.1029/2004GL019665.
Miller, S. R., S. L. Baldwin, and P. G. Fitzgerald (2012), Transient fluvial incision and active surface uplift in the Woodlark Rift of eastern Papua New Guinea, *Lithosphere*, *4*(2), 131–149.
Mohn, G., G. Manatschal, O. Muntener, M. Beltrando, and E. Masini (2010), How does the continental crust thin during rifting in magma-poor rifted margins: Evidence from the Bernina/Campo/Grosina units in the Central Alps (SE-Switzerland and N-Italy), *Int. J. Earth Sci.*, *99*, 75–101, doi:10.1007/s00531-010-0566-6.
Munguía, L., M. González, S. Mayer, and A. Aguirre (2006), Seismicity and State of Stress in the La Paz–Los Cabos Region, Baja California Sur, Mexico, *Bull. Seismol. Soc. Am.*, *96*(2), 624–636.
Nourse, J. A., T. H. Anderson, and L. T. Silver (1994), Tertiary metamorphic core complexes in Sonora, northwestern Mexico, *Tectonics*, *13*(5), 1161–1182, doi:10.1029/93TC03324.
Oskin, M., and J. Stock (2003a), Pacific–North America plate motion and opening of the Upper Delfín Basin, northern Gulf of California, Mexico, *Geol. Soc. Am. Bull.*, *115*(10), 1173–1190, doi:10.1130/B25154.1.
Oskin, M., and J. Stock (2003b), Marine incursion synchronous with plate-boundary localization in the Gulf of California, *Geology*, *31*(1), 23–26, doi:10.1130/0091-7613(2003)031<0023:MISWPB>2.0.CO;2.
Oskin, M., J. Stock, and A. Martín-Barajas (2001), Rapid localization of Pacific–North America plate motion in the Gulf of California, *Geology*, *29*(5), 459–462, doi:10.1130/0091-7613(2001)029<0459:RLOPNA>2.0.CO;2.
Páramo, P., W. S. Holbrook, H. E. Brown, D. Lizarralde, J. Fletcher, P. Umhoefer, G. Kent, A. Harding, A. Gonzalez, and G. Axen (2008), Seismic structure of the southern Gulf of California from Los Cabos block to the East Pacific Rise, *J. Geophys. Res.*, *113*, B03307, doi:10.1029/2007JB005113.
Parry, W. T., and L. M. Downey (1982), Geochemistry of hydrothermal chlorite replacing igneous biotite, *Clays Clay Miner.*, *30*(2), 81–90.
Pik, R., N. Bellahsen, S. Leroy, Y. Denèle, P. Razin, A. Ahmed, and K. Khanbari (2013), Structural control of basement denudation during rifting revealed by low-temperature (U-Th-Sm)/He thermochronology of the Socotra Island basement—Southern Gulf of Aden margin 2013, *Tectonophysics*, *607*, 17–31, doi:10.1016/j.tecto.2013.07.038.
Peccerillo, A., and S. R. Taylor (1976), Geochemistry of Eocene calc-alkaline roks from Kastamonu area, northern Turkey, *Contrib. Mineral. Petrol.*, *58*(1), 63–81.
Pérez-Venzor, J. A. (2013), Estudio geológico-geoquímico del borde oriental del Bloque de los Cabos, tesis doctoral, Univ. Nacional Autónoma de México, Baja California Sur, México.
Persaud, P., X. Pérez-Campos, and R. W. Clayton (2007), Crustal thickness variations in the margins of the Gulf of California from receiver functions, *Geophys. J. Int.*, *170*, 687–699.
Philippon, M., E. Willingshofer, D. Sokoutis, G. Corti, F. Sani, M. Bonini, and S. Cloetingh (2015), Slip re-orientation in oblique rifts, *Geology*, *43*(2), 147–150.
Plattner, C., R. Malservisi, and R. Govers (2009), On the plate boundary forces that drive and resist Baja California motion, *Geology*, *37*, 359–362, doi:10.1130/G25360A.1.
Romero, D. A. M., V. S. Unda, A. M. Rodrigues, and J. C. Aguilera Hale (2002), Carta Geologico-Minera San José Del Cabo F12-2-3-5-6, Baja California Sur, Esc. 1:250,000, map.
Schaaf, P., H. Böhnel, and J. A. Pérez-Venzor (2000), Pre-Miocene palaeogeography of the Los Cabos Block, Baja California Sur: Geochronological and palaeomagnetic constraints, *Tectonophysics*, *318*(1), 53–69, doi:10.1016/S0040-1951(99)00306-6.
Seiler, C., J. M. Fletcher, M. C. Quigley, A. J. Gleadow, and B. P. Kohn (2010), Neogene structural evolution of the Sierra San Felipe, Baja California: Evidence for proto-gulf transtension in the Gulf Extensional Province?, *Tectonophysics*, *488*, 87–109, doi:10.1016/j.tecto.2009.09.026.
Seiler, C., J. M. Fletcher, B. P. Kohn, A. J. Gleadow, and A. Raza (2011), Low-temperature thermochronology of northern Baja California, Mexico: Decoupled slip-exhumation gradients and delayed onset of oblique rifting across the Gulf of California, *Tectonics*, *30* TC3004, doi:10.1029/2009TC002649.
Spencer, J. E. (2010), Structural analysis of three extensional detachment faults with data from the 2000 Space-Shuttle Radar Topography Mission, *GSA Today*, *20*, 4–10.
Spencer, J. E. (2011), Gently dipping normal faults identified with Space Shuttle radar topography data in central Sulawesi, Indonesia, and some implications for fault mechanics, *Earth Planet. Sci. Lett.*, *308*, 267–276.
Spencer, J. E., and W. R. Normark (1979), Tosco-Abreojos fault zone: A Neogene transform plate boundary within the Pacific margin of southern Baja California, Mexico, *Geology*, *7*(11), 554–557, doi:10.1130/0091-7613(1979)7<554:TFZANT>2.0.CO;2.
Steiger, R., and E. Jäger (1977), Subcommission on geochronology: Convention on the use of decay constants in geo-and cosmochronology, *Earth Planet. Sci. Lett.*, *36*(3), 359–362.
Stock, J. M., and K. V. Hodges (1989), Pre-Pliocene extension around the Gulf of California and the transfer of Baja California to the Pacific Plate, *Tectonics*, *8*(1), 99–115, doi:10.1029/TC008i001p00099.
Sun, S.-S., and W. F. McDonough (1989), Chemical and isotopic systematics of oceanic basalts: Implications for mantle composition and processes, *Geol. Soc. London Spec. Publ.*, *42*(1), 313–345.

Sutherland, F. H. (2006), Continental rifting across the southern Gulf of California, PhD thesis, Univ. of Calif., San Diego.
Sutherland, F. H., G. M. Kent, A. J. Harding, P. J. Umhoefer, N. W. Driscoll, D. Lizarralde, J. M. Fletcher, G. J. Axen, W. S. Holbrook, and A. González-Fernández (2012), Middle Miocene to early Pliocene oblique extension in the southern Gulf of California, *Geosphere*, *8*(4), 752–770, doi:10.1130/GES00770.1.
Umhoefer, P. J. (2011), Why did the Southern Gulf of California rupture so rapidly?—Oblique divergence across hot, weak lithosphere along a tectonically active margin, *GSA Today*, *21*, doi:10.1130/G133A.1.
Umhoefer, P. J., L. Mayer, and R. J. Dorsey (2002), Evolution of the margin of the Gulf of California near Loreto, Baja California peninsula, Mexico, *Geol. Soc. Am. Bull.*, *114*(7), 849–868.
Umhoefer, P. J., T. Schwennicke, M. T. Del Margo, G. Ruiz-Geraldo, J. C. Ingle, and W. McIntosh (2007), Transtensional fault-termination basins: An important basin type illustrated by the Pliocene San Jose Island Basin and related basins in the southern Gulf of California, Mexico, *Basin Res.*, *19*, 297–322.
Umhoefer, P. J., S. J. Maloney, B. Buchanan, J. R. Arrowsmith, G. Martinez-Gutiérrez, G. Kent, N. Driscoll, A. Harding, D. Kaufman, and T. Rittenour (2014), Late Quaternary faulting history of the Carrizal and related faults, La Paz region, Baja California Sur, Mexico, *Geosphere*, *10*, 476–504, doi:10.1130/GES00924.1.
Unternehr, P., G. Péron-Pinvidic, G. Manatschal, and E. Sutra (2010), Hyper-extended crust in the South Atlantic: In search of a model, *Pet. Geosci.*, *16*, 207–215.
Whitney, D. L., C. Teyssier, P. Rey, and W. R. Buck (2013), Continental and oceanic core complexes, *Geol. Soc. Am. Bull.*, *125*, 273–298.
Wong, M. S., and P. B. Gans (2003), Tectonic implications of early Miocene extensional unroofing of the Sierra Mazatán metamorphic core complex, Sonora, Mexico, *Geology*, *31*(11), 953–956, doi:10.1130/G19843.1.
Wong, M. S., and P. B. Gans (2008), Geologic, structural, and thermochronologic constraints on the tectonic evolution of the Sierra Mazatán core complex, Sonora, Mexico: New insights into metamorphic core complex formation, *Tectonics*, *27*, doi:10.1029/2007TC002173.
Wong, M. S., P. B. Gans, and J. Scheier (2010), The $^{40}Ar/^{39}Ar$ thermochronology of core complexes and other basement rocks in Sonora, Mexico: Implications for Cenozoic tectonic evolution of northwestern Mexico, *J. Geophys. Res.*, *115* B07414, doi:10.1029/2009JB007032.
Zanchi, A. (1994), The opening of the Gulf of California near Loreto, Baja California, Mexico: From basin and range extension to transtensional tectonics, *J. Struct. Geol.*, *16*(12), 1619–1639.